

Responses to the reviewers' comment

Anonymous Referee #1

Review of “Alteration of the microphysical properties of black carbon through transport in the boundary layer in East Asia” by Takuma Miyakawa et al. submitted to Atmospheric Chemistry and Physics.

We appreciate the reviewer's helpful and constructive comments on the manuscript entitled “Alteration of the microphysical properties of black carbon through transport in the boundary layer in East Asia”. As the reviewers suggested, we have modified the manuscript. Major points for the revisions are listed as follows.

- 1) Title has been changed.
- 2) Supporting information (SI) has been prepared.
- 3) We have modified the discussion section.

*Note the reviewers' comments in **bold**.

The manuscript discusses ground-based measurements, with several instruments, of black carbon (BC) near an industrial source region and at a location removed from the source to study the effects of precipitation on the size distribution and properties of the BC-containing particles. The manuscript is well written and competently explains the study, but several of the arguments do not seem supported by the data. If the comments below are addressed I would recommend that the manuscript be accepted for publication. The title refers to "microphysical properties," which is true, but perhaps "size distribution and amount of associated non-BC material" would be more accurate, as the former term implies a host of properties that were not addressed.

>As the reviewer suggested, this study has investigated a part of the microphysical parameters of BC. Shape and chemical composition of BC-containing particles, which were not directly measured in this study, are important for considering the climatic impacts of BC-containing particles. However, chemical composition of non-refractory (non-BC) materials for both BC-free and -containing particles was measured using an Aerosol Chemical Speciation Monitor (ACSM). We addressed just simply the mixing state of BC-containing particles, and therefore revised the title slightly to “Alteration of the size distributions and mixing states of black carbon through transport in the boundary layer in East Asia”.

Line 56: The sweeping statement that "washout cannot substantially affect the

lifetime of atmospheric BC-containing particles," even with a reference to Seinfeld and Pandis, seems difficult to justify. Do the authors mean that because most of the BC-containing particles have diameters of several hundred nanometers, their ability to be scavenged by falling precipitation is not very large? This would seem to depend on the intensity of precipitation.

>As the reviewer suggested, the accumulation mode aerosols including BC are not effectively removed by the falling rain droplets. Washout process is dependent on the precipitation intensity (PI) and rain drop size as well as the particle size range. In this study, the information of rain drop size is not available. The average PIs along a backward trajectory were calculated for the rain period in 3d-backward time ($PI > 0 \text{ mm h}^{-1}$). They ranged from 0.1 to 2.5 mm h^{-1} (median = $\sim 0.6 \text{ mm h}^{-1}$). Using the PI value of 0.6 mm h^{-1} , the scavenging rates of accumulation mode particles were estimated to be $6E-3 \text{ h}^{-1}$ ($6E-5 \text{ h}^{-1}$) with the assumed rain drop diameter of 0.2 mm (2 mm). The corresponding time constants are around 7 and 694 days. These are longer than the typical transport time from the continent to the observation site. The details are described in SI.

Line 148: Rather than "lower and upper boundaries" it would be preferable to state "outside the diameter range . . ." so that it is clear what size is being referred to.

>We have revised as suggested.

Lines 152-154: Some discussion of why the EC and rBC concentrations differ, and especially why the rBC concentration is less, seems to be necessary. Line 168: Some justification for the selection of 0.5 as the collection efficiency for sulfate in the ACSM is required.

>In this study, we compared rBC with effective BC (EBC) measured using a light absorption technique (COSMOS). As we stated in the original manuscript, the difference between rBC and EBC is within the uncertainties related to both measurements. One of the unclear uncertainties, which have not well been studied, is the detection sensitivity of SP2 to the ambient rBC particles (incandescence signal intensity per rBC particle mass, $S_{LII-m_{pp}}$) in a remote atmosphere. It was found in previous studies (Moteki and Kondo, 2010; Miyakawa et al. 2016) that the $S_{LII-m_{pp}}$ relationship of fullerene soot (FS) particles, which is used as a calibration standard for the SP2, is similar to that of ambient rBC particles in urban/industrial area. We hence assume the same sensitivity of SP2 to the ambient rBC in a remote atmosphere as that

of FS particles and rBC particles in urban/industrial area. I added some explanations on the related uncertainties to the section 2.1 in the revised manuscript.

The collection efficiency of ACSM-SO₄²⁻ was derived from Yoshino et al. (2016). This paper is included in the reference list of the revised manuscript.

Line 206: Some discussion of how sensitive the results are to different choices for the percentile (i.e., does the background value change if concentrations lower than the 10th percentile were averaged?) would be helpful, or better yet, a distribution of the CO concentrations should be shown.

>When we set 10th percentile of CO mixing ratio as the threshold value, the derived background CO mixing ratio was calculated to be 131 ppb, which is slightly higher than the original value (120 ppb). We prepared SI including the descriptions on the determination of the background CO mixing ratio. Please see SI for details.

Line 277: The statement that the ACSM-SO₄ and the IC-SO₄ "generally agreed well" is true, but from Fig. 5c there appears to be little variability in either at concurrent times when comparison could be made.

>The variability in IC-SO₄²⁻ mass concentration was ~9 μg m⁻³ at STP (min - max ~1 - ~10). Wider range of concentrations (<~20 μg m⁻³) were observed during an intercomparison experiment in Queens/New York (Drewnick et al., 2003). To the best of our knowledge, the observed range was larger enough to discuss the intercomparison results. For example, Takegawa et al. (2005) reported the intercomparison results of SO₄²⁻ mass concentration between Aerodyne AMS and PILS-IC. The range given in their study (< ~7 μg m⁻³) is smaller than ours.

Line 284: It is not clear why the positive correlation of SO₄ and CO suggests that the SO₄ was secondary and that SO₄ contributed to the BC coatings; more explanation of these assumptions/conclusions is required.

>Growth of BC-containing particles should be explained separately from the formation. Besides our observation results, previous studies support the description of formation and structure of the coating of BC in the original manuscript. As the reviewer suggested, we revised the related sentences and included more explanation in the revised manuscript.

Line 290: The authors note "the small variability of SO₄/CO ratios," yet Figure 6b shows that these ratios vary considerably.

>As the reviewer suggested, this statement and Figure 6b seem to contradict each other. We removed this sentence for the clarity.

Lines 294, 297: The two "experiments," which consisted of two brief time periods out of a month of data, were used to justify conclusions regarding flow patterns. While the results are indeed consistent with the arguments made, it seems difficult to justify such conclusions on the basis of one comparison.

>As the reviewer suggested, the results shown in this study are based on the observation during not-so-long time periods. We agree that it is actually difficult to draw the general conclusions. However, we still believe that this paper shows the significance in the observational studies of the relationship between removal process and the changes in the BC microphysical properties, because the observed meteorological conditions in the spring of 2015 were not special and similar to those with an average year. We added the sentences "The migrating anticyclone and cyclone were observed during this period, which is typically dominant in spring over East Asia (Asai et al., 1988). We here only briefly describe the meteorological fields (wind flow and precipitation) in the following." behind the first sentence in section 3.1, and modified the last sentence in section 3.5 to "As the results from this study are based on observations during a limited length of time, it would be worthwhile to further investigate the possible connections of the variabilities in BC microphysical properties and meteorological conditions in this region to provide useful constraints on more accurate evaluations of climatic impacts of BC-containing particles (Matsui, 2016)". Please see the revised manuscript for details.

Line 317: The authors refer to the SO₄/CO ratio, but does this really refer to the deltaSO₄/delta-CO ratio? It was unclear to me here and a number of places elsewhere in the text whether the CO and SO₄ values referred to delta-CO and delta-SO₄ values or not. For clarity, I would recommend using "delta-" values throughout.

>We clearly found the lower concentrations of SO₄²⁻ relative to CO for the data with the higher APT in Figure 6b of the original manuscript. Another reason not to include the $\Delta\text{SO}_4^{2-}/\Delta\text{CO}$ ratio is the uncertainty related to the variability in the background of SO₄²⁻ in East Asia. Although the use of the same data treatment would be clear for the readers, we did not quantitatively analyze the hourly ΔSO_4^{2-} and ΔCO values for considering the relative enhancements of SO₄²⁻ to CO in this study. We hence added the sentences to explain why we do not analyze Δ values in the revised manuscript in

section 2.2.

Lines 317-319: The difference in slopes shown in the inset to Figure 6b doesn't seem sufficiently large, given the scatter of the data, to be significantly different, and certainly not to justify the conclusion that the controlling process is rainout.

>The rainout lowered the transport efficiency of SO_4^{2-} as well as BC (to CO). However, the cloud process not associated with the precipitation can affect the relative increases of SO_4^{2-} concentration. The major purpose to include this figure is to elucidate the impact of the cloud process on the aqueous-phase formation of SO_4^{2-} , and is not to discuss the loss processes. Figure 6b is modified in the revised manuscript to clarify the data points with the APT of zero (no precipitation through the transport). These data points are highlighted by marking using cross markers. Please see the revised Figure 6b for details.

Line 343: Here and elsewhere the argument is made that aging leads to growth of BC particles, which is well accepted, but such aging can also lead to loss of larger particles through rainout, yet size distributions in Figure 7 doesn't show much of a difference between size distributions for air masses with BC loss and those without, and certainly not more of a difference for larger BC particles than for smaller ones. This discrepancy requires explanation.

>All the size distributions shown in Figure 7 are normalized by the number or mass integrated for the measured size range, which is described in the caption of this figure. The "absolute" size distributions show more differences between with and without BC loss. We modified the size distributions from "normalized" to "absolute" and added a new figure (fig 7c of the revised manuscript) of the relationship between BC peak diameters and $\Delta\text{BC}/\Delta\text{CO}$ (i.e., degree of the removal of BC). This figure clarifies the significance of the observed changes in the peak diameter. Please see the revised figure for more details.

Line 345: The statement that "small BC-containing particles were scavenged by larger particles in the coagulation process" is a hypothesis, but stated as truth. It would seem that concentrations are too low for much coagulation over the brief period (a few days), especially for particles that are many tens of nanometers in diameter. Calculations or a simple model would be required to support this hypothesis. Line 353: It would be preferable, and less ambiguous, to rephrase "BC size of 0.2" to "BC diameter of 0.2".

>In the consideration of the washout process, the removal of small BC-containing particles through the washout is expected to be significant as well as the coagulation process. We hence describe the possibility of both processes in the revised manuscript. We rephrased “BC size of 0.2” to “BC diameter of 0.2”.

Line 368: The discussion focused on transport pathways of particles in the particular region of the study, but I was expecting more discussion on the results, what they mean, and so forth. There seemed to be little relevance to the second paragraph of the discussion.

>We reorganized the discussion part (section 3.5). We merged and reorganized the first paragraph and the half of the second paragraph into one paragraph. The latter half of the first paragraph of section 3.5 discusses the observed features and its relevance to the finding in previous studies. We consider that the relationship between transport pathways (i.e., processes during transport) and its impact on the aerosol particles is a key and relevant to our observation results. We hence modified the sentences of the third (second in the revised manuscript) paragraph.

Line 372: The decrease in the peak diameter of the mass size distribution is very small, and within uncertainty.

>The change in the peak diameter is small, however, significant. Corresponded change in BC mass is ~1 fg/particle. This difference can be resolved by the SP2 and beyond the uncertainty. The variabilities of the peak diameters are summarized in Table 1 in the original and revised manuscript and are smaller than those measured. As we described in the above, we added a new figure to show the tendency of the BC particle diameter as a function of the degree of BC removal (Fig 7c of the revised manuscript).

Line 373: The statement that the evidence implies selective removal of large BC containing particles is not supported by Figure 7, which shows a very slight difference in the size distribution between "with BC loss" and "without BC loss" but not apparent selective decrease of larger particles. If there were selective removal, I would expect the size distribution to not be lognormal, but to have a deficit on the large side below what a lognormal would be. Figure 3a is very difficult to read; could it be made larger? Figure 3b requires units for q_v to accompany the scale. Figure 4a should be made larger also, if possible. Figure 5b: it is difficult to distinguish the COSMOS and SP2 BC values; perhaps make one

red and the other black? Figure 6a: do the axes refer to delta-CO and delta-BC? If so, they should be labeled as such. Figure 6b, inset: what does "all data" refer to? If this is to label the gray dot, then it is not clear.

>The activation of aerosol particles to cloud droplets has occurred during transport. We did not observe the aerosol particles below the convective cloud, because the migratory cyclone was the dominant process for the upward transport in spring in East Asia. We thus considered that SP2 detected BC-containing particles which have been aged (about a half ~ a day, typical transport time) since affected by the wet removal. The size distributions of BC-containing particles can change during transport again after the rainout process, and therefore do not always conserve the original shape.

We have corrected some figures as suggested. We enlarged all figures as large as possible as suggested. Units of all parameters in Fig 3 were clarified in the modified one. The color of SP2-BC in Fig 5 was changed to red. Axes of Fig 6a do not refer to delta (so we didn't change). Fig 6b was modified, because it was not clear. All the values in Figure 6 are absolute concentrations (not delta). Fig 7c was newly added (Please see the texts for details).

References

- Asai, T., Y. Kodama, and J.-C. Zhu (1988), Long-term variations of cyclone activities in East Asia, *Adv. Atmos. Sci.*, 5, 149–158.
- Drewnick, F., Schwab, J. J., Högrefe, O., Peters, S., Husain, L., Diamond, D., Weber, R., and Demerjian, K. L. (2003), Intercomparison and Evaluation of Four Semi-Continuous PM_{2.5} Sulfate Instruments, *Atmos. Environ.*, 37:3335–3350.
- Matsui, H., Black carbon simulations using a size- and mixing-state-resolved three-dimensional model: 1. Radiative effects and their uncertainties (2016), *J. Geophys. Res. Atmos.*, 121, 1793–1807, doi:10.1002/2015JD023998
- Takami, A., et al. (2013), Structural analysis of aerosol particles by microscopic observation using a time-of-flight secondary ion mass spectrometer, *J. Geophys. Res. Atmos.*, 118, 6726–6737, doi:10.1002/jgrd.50477.
- Takegawa, N., Miyazaki, Y., Kondo, Y., Komazaki, Y., Miyakawa, T., Jimenez, J. L., Jayne, J. T., Worsnop, D. R., Allan, J. D., and Weber, R. J. (2005), Characterization of an Aerodyne Aerosol Mass Spectrometer (AMS): Intercomparison with Other Aerosol Instruments, *Aerosol Sci. Technol.*, 39:760–770.
- Yoshino, A., A. Takam, K. Sato, A. Shimizu, N. Kaneyasu, S. Hatakeyama, K. Hara, and M. Hayashi (2016), Influence of Trans-Boundary Air Pollution on the Urban

Atmosphere in Fukuoka, Japan, *Atmosphere*, 7, 51, doi:10.3390/atmos7040051.

Referee #2 Dr. Gavin McMeeking

Review of Miyakawa et al.

We appreciate your helpful and constructive comments on the manuscript entitled “Alteration of the microphysical properties of black carbon through transport in the boundary layer in East Asia”. As the two reviewers suggested, we have modified the manuscript. Major points for the revisions are listed as follows.

- 1) Title has been changed.
- 2) Supporting information (SI) has been prepared.
- 3) We have modified the discussion section.

*Note the reviewers' comments in **bold**.

The authors present a one month case study examining measurements of black carbon properties at a remote island site, using co-located measurements of CO and sub-micron aerosol composition and reanalysis data to evaluate precipitation impacts on the observed properties. The manuscript focuses on contrasting observed properties during periods with differing accumulated precipitation along backward trajectories. The paper is well prepared and well organized and the subject is well within the topic area for ACP. There are several areas where minor revisions are needed, however, before the paper can be recommended for publication. I agree with the points raised by Reviewer #1, so have tried to not repeat too much of what has been already raised. The comments should be addressed in a revised manuscript. In addition:

+ Given the focus of the manuscript, the introduction would benefit from a more thorough discussion of the various BC removal mechanisms, with more mechanistic details given as to why various processes may or may not be important in the study area. Distinction should be made between in-cloud processes (nucleation scavenging versus scavenging by pre-existing droplets), below-cloud (washout) and dry deposition.

We added the sentence describing the removal processes of BC to the second paragraph of section “Introduction”. Relate to this, as the reviewer #1 suggested, we have modified the descriptions on the relative importance of the washout (to the rainout) (in section 3.3 of the original manuscript). A previous study (Kanaya et al., 2016) is referred for quantitatively elucidating the impacts of dry deposition. The timescale of the removal through the washout was evaluated in this study to be longer than the typical time scale of the transport (details in S.I. newly-prepared). Please see the

revised manuscript and SI for more details.

+ Two points regarding reported SP2-measured BC number/mass distributions. First, the manuscript needs to make it more clear when BC core versus shell diameters are being discussed, especially when linking the observations to theory. For example, while it is true we would expect larger particles to be removed in air masses heavily impacted by precipitation, the effects on BC core distributions will be confounded by other material mixed with the cores. Related to this, the diameter range for which the optical sizing of the BC particles should be provided in the methods section. Second, small changes in the detection efficiency of the SP2 at its lower limit due to changes in cavity laser power can look like changes in BC core number distribution. A short statement regarding any checks on cavity laser power or other approaches used to ensure consistent behavior at lower size limits for the instrument would be useful.

As the reviewer suggested, we added explanations on these SP2 working conditions in section 2.1. Please see the revised manuscript for more details.

+ Potentially useful additional information provided by the ACSM is being ignored by examining only sulfate. Is there a reason for this?

>We analyzed the concentration of SO_4^{2-} measured using the ACSM for the reasons, (1) “its precursor gas (sulfur dioxide) shares the emission sources and locations with CO”, and (2) “its formation process in the aqueous phase reaction is useful for analyzing the effect of a possible cloud processing through air parcel transport”. We added more explanations especially on (2) to section 2.1.

References

Kanaya, Y., X. Pan, T. Miyakawa, Y. Komazaki, F. Taketani, I. Uno, and Y. Kondo (2016), Long-term observations of black carbon mass concentrations at Fukue Island, western Japan, during 2009-2015: Constraining wet removal rates and emission strengths from East Asia, *Atmos. Phys. Chem.*, 16, 10689-10705, doi:10.5194/acp-16-10689-2016, 2016

1 **Alteration of the ~~microphysical properties~~size distributions**
2 **and mixing states of black carbon through transport in the**
3 **boundary layer in East Asia**

4
5 Takuma Miyakawa^{1,2}, Naga Oshima³, Fumikazu Taketani^{1,2}, Yuichi Komazaki¹, Ayako
6 Yoshino⁴, Akinori Takami⁴, Yutaka Kondo⁵, and Yugo Kanaya^{1,2}

7 ¹Department of Environmental Geochemical Cycle Research, Japan Agency for
8 Marine-Earth Science and Technology, 3173-25 Showa-machi, Kanazawa-ku,
9 Yokohama, Kanagawa, 236-0001, Japan.

10 ²Institute for Arctic Climate Environment Research, Japan Agency for Marine-Earth
11 Science and Technology, 3173-25 Showa-machi, Kanazawa-ku, Yokohama, Kanagawa,
12 236-0001, Japan.

13 ³Meteorological Research Institute, 1-1 Nagamine, Tsukuba, Ibaraki, 305-0052, Japan

14 ⁴Center for Regional Environmental Research, National Institute for Environmental
15 Studies, 16-2 Onogawa, Tsukuba, Ibaraki, 305-8506, Japan

16 ⁵National Institute for Polar Research, 10-3 Midori-cho, Tachikawa, Tokyo, 190-8518,
17 Japan

18 *Correspondence to:* Takuma Miyakawa (miyakawat@jamstec.go.jp)

19
20 **Abstract.** Ground-based measurements of black carbon (BC) were performed near
21 an industrial source region in the early summer of 2014 and at a remote island in Japan
22 in the spring of 2015. Here, We-we report on the temporal variations in the transport,
23 size distributions, and mixing states of the BC-containing particles. These particles

24 | ~~were characterized-measured by~~ using a continuous soot monitoring system, a single
25 | particle soot photometer, and an aerosol chemical speciation monitor. The effects of
26 | aging on the growth of BC-containing particles were examined by comparing the
27 | ground-based observations between the near-source and remote island sites.
28 | Secondary formation of sulfate aerosols through gas- and cloud-phase reactions
29 | strongly affected the increases in BC coating (i.e., enhancement of cloud condensation
30 | nuclei activity) with air mass aging from the source to the outflow regions. The
31 | effects of ~~the~~ wet removal on ~~the~~ BC microphysics were elucidated by classifying the
32 | continental outflow air masses depending on the enhancement ratios of BC to CO
33 | ($\Delta\text{BC}/\Delta\text{CO}$) ~~ratios, which were used~~ as an indicator of the transport efficiency of BC.
34 | ~~It was found~~ The findings showed that $\Delta\text{BC}/\Delta\text{CO}$ ratios were controlled mainly by the
35 | rainout process during transport in the planetary boundary layer (PBL) on the timescale
36 | of 1–2 days. The meteorological conditions and backward trajectory analyses
37 | suggested that air masses strongly affected by rainout originated mainly from a region
38 | in Southern China ~~region~~ (20°–35°N) ~~during this season~~ in the spring. Selective
39 | removal of large and thickly-coated BC-containing particles was ~~found-detected~~ in the
40 | air masses that were substantially affected by the rainout in the PBL, as predicted by
41 | Köhler theory. The size and water-solubility of BC-containing particles in the PBL
42 | can be altered by the rainout process as well as the condensation of non-BC materials.

43

44 | 1. Introduction

45 | Black carbon (BC)-containing particles in the atmosphere can significantly affect the
46 | radiative budget of the Earth through two types of effects; namely, direct (light
47 | absorption and scattering) effect and indirect (aerosol–cloud interactions) effects
48 | (Bond et al., 2013; references therein). The difficulty in the estimation of these

49 effects in the atmosphere results from both the short lifetime of BC-containing
50 particles relative to other greenhouse gases and the variable physicochemical
51 properties of ~~BC-containing~~such particles. The BC itself is water-insoluble
52 immediately after emission, but it subsequently ~~takes exhibits on~~ hygroscopicity
53 (McMeeking et al., 2011) and cloud condensation nuclei (CCN) activity (Kuwata et al.,
54 2007) ~~through following~~ atmospheric transport and aging. Only small amounts of
55 water-soluble materials on BC particles are needed ~~for to cause~~ their activation,
56 ~~whereby they will to~~ form cloud droplets under moderate supersaturation conditions
57 (Kuwata et al., 2007; 2009). ~~It is considered that~~The BC-containing particles are
58 ~~thought to be~~ removed from the atmosphere mainly by ~~the rainout wet~~
59 ~~deposition process. This is because other removal processes such as gravitational~~
60 ~~settling, dry deposition, and washout cannot substantially affect the lifetime of~~
61 ~~atmospheric BC-containing particles~~ (Seinfeld and Pandis, 2006).

62 The horizontal and vertical distributions of aerosols can be substantially altered by
63 their atmospheric lifetimes (e.g., Lawrence et al., 2007). Moreover, their studies
64 suggested that ~~The removal processes of BC such as dry deposition, below-cloud (i.e.,~~
65 washout), and in-cloud (i.e., rainout) processes can greatly change the atmospheric
66 lifetimes. The in-cloud processes include nucleation scavenging and scavenging by
67 the preexisting cloud droplets. Precipitation followed by in-cloud process leads to the
68 irreversible removal of BC-containing particles. Samset et al. (2014), using multiple
69 global model data sets constrained by aircraft observations, suggested that the
70 atmospheric lifetime of BC largely affects its distribution, especially in the northern
71 hemisphere, and this resulting results in significant variations in global direct radiative
72 forcing values. The removal of BC has been considered to be an important issue for

73 | the geochemical carbon cycle as well as for climate sciences. The BC-containing
74 | particles deposited onto the ocean surface can affect ocean surface particles, dissolved
75 | organic carbon (DOC), and microbial processes; by-via absorbing DOC, stimulating
76 | particle aggregation, and changing the size distribution of suspended particles (Mari et
77 | al., 2014).

78 | Previous modeling studies have dealt with ~~the~~ BC aging processes (condensational
79 | growth and coagulation) in box and regional-scale models, and parameterized
80 | timescales for the conversion of BC-containing particles from water-insoluble to -
81 | soluble ~~for-in~~ global models (Oshima et al., 2009; Liu et al., 2011; Oshima and Koike,
82 | 2013). However, Quantitative—quantitative knowledge of the variability of
83 | microphysical parameters of BC-containing particles and the timescale of their aging
84 | processes is still limited, and thus is-more data are needed for near-source and remote
85 | regions (Samset et al., 2014). Moteki et al. (2012) reported the first observational
86 | evidence of the size-dependent activation of BC ~~to-during the formation of~~ cloud
87 | droplets, in air masses uplifting from the planetary boundary layer (PBL) to the free
88 | troposphere (FT) in East Asia in-during the spring of 2009, during-as part of the
89 | Aerosol Radiative Forcing in East Asia (A-FORCE) aircraft campaigns (Oshima et al.,
90 | 2012). The-A similar altitude dependence of the BC size distribution and-similarity-in
91 | the-BC mixing state were-was observed in other aircraft measurements conducted in
92 | East Asia in-during the winter (Kondo et al., 2016). Selective removal of larger
93 | BC-containing particles through the cloud process, which is predicted by Köhler theory,
94 | was qualitatively observed in the atmosphere. This observational evidence indicates
95 | that the size distributions and mixing states of BC-containing particles control the
96 | global- and regional-scale spatial distributions of BC through their upward transport

97 | from the PBL to the FT ~~in associated~~ association with rainout processes. Despite the
98 | importance of the size distributions and mixing states of BC-containing particles in the
99 | PBL, the ~~continuous~~ measurements of their microphysical properties are still limited
100 | around the source regions in East Asia.—

101 | Kanaya et al. (2016) have conducted long-term measurements of BC for 6 years
102 | (2009—2015) at Fukue Island, and ~~they~~ synthetically reported on the emission and
103 | removal of BC in East Asia by using these data sets. ~~It was found in their study, they~~
104 | found that wet removal through transport in the PBL substantially reduced the
105 | transport efficiency of BC aerosols. Here, we examine the effects of aging and wet
106 | removal during transport on the changes in BC size distributions and mixing state, as
107 | well as concentrations, based on ground-based measurements taken at the same site in
108 | the spring of 2015 by using a single particle soot photometer (SP2) and an Aerosol
109 | Chemical Speciation Monitor (ACSM). We first ~~describes~~ show the meteorological
110 | characteristics of the East Asian region in the spring of 2015. ~~Then, We discuss the~~
111 | relative importance of below cloud the washout and rainout in cloud processes for the
112 | wet removal of BC as well as the transport patterns of the East Asian outflow air
113 | masses in spring. ~~Then~~ Lastly, the loss of BC-containing particles for that period is
114 | investigated by using a similar approach to that used by Kanaya et al. (2016), and this
115 | is performed in connection with the associated changes in BC microphysics and their
116 | relevance with to the transport pathways.

117 |

118 | 2. Experimental and data analysis

119 | 2.1. Atmospheric ~~Observations~~ observations

120 | ~~The c~~ ontinuous measurements of PM_{2.5} and BC aerosols ~~has~~ have been conducted
121 | at a remote island, Fukue Island, since February 2009 (Kanaya et al., 2013; Ikeda et al.,

122 2014). The observation site is located at the Fukue Island Atmospheric Environment
123 Monitoring Station (32.75°N, 128.68°E, **Fig. 1**), and ~~The-the~~ site is ~~located-situated~~
124 in the northwest portion of Fukue Island, approximately 20 km from the main
125 residential area in the southeast. The fine mode aerosols sampled at the site are
126 mostly transported from areas beyond the island. The enhanced concentrations of BC
127 aerosol ~~detected at~~ Fukue Island ~~are-can be~~ mainly attributed to long-range transport
128 from the Asian continent, according to a previous study (Shiraiwa et al., 2008) and an
129 emission inventory work (**Fig. 1**, REAS ver. 2.1, Kurokawa et al., 2013).

130 We deployed an SP2 (Droplet Measurement Technologies, Inc., USA) for the
131 analysis of microphysical parameters of refractory BC (rBC, Petzold et al., 2013) from
132 March 26, 2015 to April 14, 2015. The SP2 was calibrated before starting the
133 ambient measurements. The calibration protocol for our SP2 is described in
134 Miyakawa et al. (2016). Fullerene soot (FS, stock 40971, lot L20W054, Alfa Aesar,
135 USA) particles were used as a calibration standard for the SP2. The variations in the
136 laser power were within $\pm 3\%$ during the observation period, thus indicating that the
137 fluctuations of laser power did not largely affect the lower limit of the detectable BC
138 size of the SP2. The ~~Mass-mass~~ equivalent diameter (MED) was derived from the
139 rBC mass per particle (m_{pp}) with ~~the an~~ assumed particle density ~~of-for~~ BC (1800 kg
140 m^{-3} , Bond and Bergstrom, 2006). A large diameter Nafion dryer (MD-700, Perma
141 Pure, Inc., USA) was placed in front of the SP2 ~~for-to~~ drying the sample air without
142 significant loss of the aerosol particles greater than 50 nm. The dry air for MD-700
143 was generated by a heatless dryer (HD-2000, Perma Pure, Inc., USA) and a
144 compressor (2AH-23-M222X, MFG Corp., USA). The relative humidity of the
145 sample air was less than 20% during the observation period. The hourly

書式変更: フォント : Times New Roman

146 number/mass size distributions and hourly median values of shell (D_S) to rBC diameter
147 (D_{core}) ratios (D_S/D_{core}) for the selected D_{core} ranges were calculated. The retrievals of
148 D_S from the light scattering signals measured by an avalanche photodiode and a
149 position sensitive detector (Gao et al., 2007) were performed by using ~~a—the~~
150 time-resolved scattering cross section method given by Laborde et al. (2012). In this
151 study, we analyzed the D_S of BC-containing particles with the D_{core} range between
152 0.15 and 0.35 μm . We also analyzed the microphysical parameters of rBC particles
153 that were measured by using the SP2 in the early summer of 2014 at Yokosuka
154 (35.32°N, 139.65°E, **Fig. 1**), which is located near industrial sources ~~beside—along~~
155 Tokyo Bay (Miyakawa et al., 2016). These data sets were used as a reference for the
156 BC-containing particles in air masses strongly affected by combustion sources.

157 Equivalent BC (EBC, Petzold et al., 2013) mass concentrations ~~are—were~~
158 continuously measured at Fukue Island by using two instruments; a continuous
159 soot-monitoring system (COSMOS₃; model 3130, Kanomax, Japan); and a multi-angle
160 absorption photometer (MAAP₃; MAAP5012, Thermo Scientific, Inc., USA). The
161 details of the air sampling and intercomparison_z for EBC measurements at Fukue
162 Island have been described elsewhere (Kanaya et al., 2013; 2016). In this study, mass
163 concentrations of EBC measured by using the COSMOS were evaluated by
164 comparison with those of SP2-derived rBC. The intercomparison between SP2 and
165 COSMOS ~~will be~~ is briefly discussed ~~in the following~~ below.

166 **Figure 2** depicts the correlation between COSMOS-EBC and SP2-rBC hourly mass
167 concentrations. ~~The—the~~ unmeasured fraction of the rBC mass was corrected by
168 extrapolation of the lognormal fit for the measured mass size distributions, to the
169 outsides of the measurable D_{core} range ~~lower and upper boundaries~~ (0.08 — and 0.5 μm ;

170 ~~respectively~~). Note that the uncertainty with respect to the unmeasured fraction of
171 rBC mass was minor (<5%) in this study. The linear regression slope of the
172 correlation between EBC and rBC was 0.88 (± 0.03). Uncertainty with respect to the
173 calibration was examined in an industrial region and found to be within around 3%
174 (Miyakawa et al., 2016). The average discrepancy between EBC and rBC was
175 beyond the uncertainty of the calibration and was comparable to the uncertainty of
176 COSMOS (10%) as evaluated by Kondo et al. (2009). ~~As~~ While the validity of the
177 calibration standard, FS particles, has been evaluated only near source regions (Moteki
178 and Kondo, 2011; Miyakawa et al., 2016), the discrepancy can be partly attributed to
179 the differences in physicochemical properties between ambient BC in remote air and
180 FS particles. Onsite calibration of the SP2 using ambient BC particles prepared by a
181 thermal denuder and particle mass classifier, such as an aerosol particle mass analyzer
182 (APM), is desirable for ~~the~~ better quantification of the rBC mass based on the
183 laser-induced incandescence technique in ~~a~~ remote areas. Although we need to make
184 further attempts to evaluate SP2 in remote areas, the data derived from this study
185 ~~suggested—indicated~~ that SP2-rBC mass concentrations agreed well with
186 COSMOS-EBC values within the ~~uncertainty—uncertainties of—~~ COSMOS.
187 ~~Therefore~~ Thus, ~~w~~ e simply use “BC”, ~~—~~ here instead of the EBC and rBC defined
188 depending upon the measurement techniques. We analyzed the COSMOS data for
189 the BC mass concentrations, and the SP2 data for the BC microphysics.

190 The chemical composition of non-refractory submicron aerosols was measured by
191 using an Aerodyne Aerosol Chemical Speciation Monitor (ACSM, Aerodyne, Inc.,
192 USA) placed in an observatory container at Fukue Island during the observation
193 period. The details of the ACSM at Fukue Island have been described in Irei et al.

194 (2014). The collection efficiency (CE) of the ACSM was assumed to be 0.5 for this
195 period ([Yoshino et al., 2016](#)). We considered sulfate (~~SO₄²⁻~~) ions (SO₄²⁻) ~~as to be the~~
196 major non-BC material and ~~the~~ most important secondary aerosols in East Asia
197 (Takami et al., 2007) for the data interpretation. The fact that SO₄²⁻ is produced in the
198 cloud phase as well as the gas phase is a benefit to for interpreting temporal changes
199 in SO₄²⁻ concentration associated with the wet removal process. During the period
200 April 1—7, 2015, the critical orifice of the inlet assembly of the ACSM ~~was~~ became
201 clogged. Therefore, the ACSM-derived SO₄²⁻ (ACSM- SO₄²⁻) for this period ~~was~~ is not
202 used in the analysis.

203 Two high volume air samplers (HV500F, Sibata Scientific Technology, Ltd., Japan)
204 were deployed on the rooftop of the observatory container. The sampling flow rate
205 for both samplers was 500 liters per minute (lpm). Air sampling was carried out for
206 21 h (from 10:00 AM to 7:00 AM) on a 110-mm pre-combusted (900°C for 3 h) quartz
207 filter (QR-100, Advantec Toyo Kaisha Ltd., Japan). Both have a PM_{2.5} impactor for
208 classifying the particle size. One impaction plate was coated with vacuum grease
209 (HIVAC-G, Shin-Etsu Chemical Co., Ltd., Japan) to minimize the impact of coarse
210 mode particles on the chemical analysis of fine mode particles, such as during
211 radiocarbon analysis, and a pre-combusted quartz fiber filter with slits was set on
212 another impaction plate to collect the coarse particles. Water soluble ions were
213 analyzed by using ion chromatography (IC, Dionex ICS1000, Thermo Fisher Scientific
214 K.K., Japan). The results from the chemical analysis of filter samples are not
215 ~~included~~ discussed in this study in detail. We only used the mass concentration of
216 sulfate ions (IC-SO₄²⁻) in this study to evaluate the uncertainty in relation to CE of the
217 ACSM, and to analyze the temporal variations during the period when the

218 ACSM-SO₄²⁻ data ~~were~~ not available (April 1–7, 2015).

219 The carbon monoxide (CO) mixing ratio ~~was~~ also continuously measured ~~by~~ using
220 a nondispersive infrared (NDIR) CO monitor (model 48C, Thermo Scientific, Inc.,
221 USA). Details of ~~the~~ CO measurements including the long-term variations in
222 sensitivity and zero level are discussed elsewhere (Kanaya et al., 2016).

223

224 2.2. Enhancement ratio of BC ~~and SO₄²⁻~~ to CO as an indicator of the BC 225 ~~removal~~transport and transformation of aerosol particles

226 In order to quantify the extent of the removal of BC, we calculated the hourly
227 enhancement ratio of BC mass concentrations to CO mixing ratios ($\Delta BC/\Delta CO$) against
228 the East Asian background air concentrations as follows:

229

$$230 \frac{\Delta BC}{\Delta CO} = \frac{[BC] - [BC]_{bg}}{[CO] - [CO]_{bg}}, \quad (1)$$

231

232 where [BC] and [CO] are measured hourly concentrations of the BC and CO,
233 respectively, and [BC]_{bg} and [CO]_{bg} are their estimated background concentrations.
234 Here, we assumed that [BC]_{bg} is zero (Oshima et al., 2012). The background
235 concentration of CO during the analysis period (March 11—April 14, 2015) was
236 calculated by averaging the concentrations lower than the 5th percentile (120 ppb).

237 The validity of this value was discussed in the supporting information (S.I.).

238 Relative changes in SO₄²⁻ to CO were also analyzed by using the linear regression
239 slopes of their correlation in this study. We ~~have~~ did not calculated the hourly
240 $\Delta SO_4^{2-}/\Delta CO$ values, because it ~~was~~ difficult to determine the background

書式変更: フォント : 太字

書式変更: インデント : 最初の行 : 1
字

241 concentration of SO₄²⁻. Analyzing the slope of the SO₄²⁻-CO correlation is
242 beneficial to the investigation of the formation processes as well as the removal
243 processes of SO₄²⁻. Especially, the aqueous-phase formation of SO₄²⁻ in clouds is
244 discussed by using this parameter.

書式変更: フォントの色 : 自動

書式変更: フォントの色 : 自動

書式変更: フォントの色 : 自動

245

246 2.3. Meteorological field analysis

247 We used the 6-hourly meteorological data, with a resolution of 1° in terms of the
248 latitude and longitude, from the National Centers for Environmental Prediction
249 (NCEP) Final (FNL) operational global analysis; ~~and~~ along with daily precipitation
250 data, with a resolution of 1° in terms of the latitude and longitude, from the Global
251 Precipitation Climatology Project (GPCP) data set (Huffman et al., 2001). We
252 analyzed these data sets to investigate the general features of the meteorological field
253 in East Asia during the observation period.

254

255 2.4. Backward trajectory analysis

256 We calculated backward trajectories from the observation site to elucidate the impact
257 of the Asian outflow. ~~3~~ Three-day backward trajectories from the observation site (the
258 starting altitude was 0.5 km) were calculated every hour by using the National Oceanic
259 and Atmospheric Administration (NOAA) Hybrid Single-Particle Lagrangian
260 Integrated Trajectory model (Draxler and Rolph, 2012; Rolph, 2012) ~~with~~ and the
261 meteorological data sets (NCEP's Global Data Assimilation system, GDAS). In this
262 study, the residence time over specific source regions was used as an indicator of their
263 impacts on the observed air masses. We defined five domains for assessing the
264 impact over the Asian continent; Northeast China (NE), Korea (KR), Central North

265 China (CN), Central South China (CS), and Japan (JP) (**Fig. 1**). The period when air
266 masses passed over the domains NE, KR, CN, and CS at least for one hour is defined
267 as that of “continental outflow”. The impacts of precipitation on the observed air
268 masses were assessed by a parameter referred to as the “Accumulated Precipitation
269 along Trajectory” (APT, Oshima et al., 2012). In this study, we calculated the APT
270 values by integrating the amount of hourly precipitation in the Lagrangian sense along
271 each 3-day back trajectory of the sampled air masses. The hourly variations of APT
272 were merged into the observed gas and aerosol data sets.

273

274 **3. Results and discussion**

275 **3.1. The meteorological field in the spring of 2015**

276 The mean meteorological field during the observation period (March 11–April 14,
277 2015) is discussed for the purpose of characterizing the general features of the wind
278 flow and precipitation in this region. The migrating anticyclone and cyclone were
279 observed during this period, which is typically dominant in spring over East Asia (Asai
280 et al., 1988). The meteorological conditions over East Asia during the observation
281 period were generally usual.—We here only briefly describe the meteorological fields
282 (wind flow and precipitation) in the following. **Figure 3a** shows the mean sea level
283 pressure (SLP) and mean horizontal winds at the 850 hPa level in East Asia during the
284 observation period. The mean equivalent potential temperature (θ_e) and the
285 meridional moisture transport at the 850 hPa level during the same period are also
286 shown in **Figure 3b**. The mid-latitude region (35–50°N, 120–140°E) was under the
287 influence of a modest monsoonal northwesterly flow, which advected cold, dry air
288 from the continent to the observation area. The subtropical region (20°–30°N, 110°–
289 -130°E) was under the influence of a persistent southwesterly flow, part of which was

290 | conversing into the observation area (30° – 35° N), ~~and this flow was being~~ confluent
291 | with the northwesterlies from the continent. The low-level southerly flow advected
292 | warm, moist air into the observation area, ~~which produced to sustain~~ a large amount of
293 | precipitation (**Fig. 4a**).—

294 | **Figure 3c** shows the temporal variations in surface pressure and precipitable water
295 | at the observation site. The surface pressure ~~is was~~ well anti-correlated with the
296 | precipitable water. During the observation period, migratory cyclones and
297 | anticyclones occurred occasionally (3 times each). The occurrence of migratory
298 | cyclones advected moist air, which could ~~have contributed~~ to the wet removal of BC
299 | during transport in the PBL. In contrast, the occurrence of anticyclones advected dry
300 | air, which could ~~have contributed~~ to the efficient transport of BC from the source
301 | regions.

302 | **Figure 4a** depicts the mean precipitation over East Asia during the observation
303 | period. Mean precipitation showed a latitudinal gradient over eastern China and the
304 | Yellow Sea and East China Sea region (i.e., increasing precipitation from ~~South-south~~
305 | to ~~North-north~~), ~~and these results~~ suggesting that transport pathways can greatly affect
306 | the wet removal of aerosols. The APT was compared with the averaged latitude of
307 | each trajectory for 48 h backwardly from the time of -24 h (Lat_{ORIG}) (**Fig. 4b**), ~~which~~
308 | ~~and these data~~ can be interpreted as an indicator ~~for-of~~ the latitudinal origin of ~~the~~ air
309 | masses arriving at Fukue Island. The high APT values corresponded to ~~the~~ air masses
310 | ~~that~~ originated from ~~the~~ southern regions (20° – 40° N). The data points are colored
311 | according to the maximum ~~relative humidity (RH)~~ values along each backward
312 | trajectory (RH_{max}). The lower RH_{max} were observed in the air masses with low APT
313 | values ~~and-that~~ originated from ~~the~~ northern regions (30° – 50° N). These air mass

314 characteristics ~~are~~ were consistent with the mean precipitation field (**Fig. 4a**). Some
315 of the data points showed high values of RH_{\max} (~100%) when their APT was almost
316 zero. These data ~~would probably~~ correspond to the air masses that experienced cloud
317 processes not associated with precipitation. Possible effects of cloud processes
318 without precipitation on the removal of aerosol particles during transport will be
319 discussed by using these data points in the following section.

320

321 **3.2. Temporal variations in BC, SO_4^{2-} , and CO**

322 Temporal variations in the concentrations of BC (measured by using COSMOS and
323 SP2), SO_4^{2-} (measured by using ACSM and IC), and CO are shown in **Figure 5**
324 ~~(middle and bottom panels respectively)~~. ACSM- SO_4^{2-} generally agreed well with
325 IC- SO_4 , thus indicating that the assumed CE (0.5) was valid for the observation period.
326 In general, BC and SO_4^{2-} were positively correlated with CO at Fukue Island, and these
327 results illustrateshowing the impact of continental outflow affected by incomplete
328 combustion sources ~~for on~~ aerosol mass concentrations. **Figure 5** also includes the
329 temporal variations in the fractional residence time over the selected region defined in
330 section 2.4 (top panel). The CO concentrations were typically enhanced for the
331 period with the higher contributions of CN and CS. ~~A previous study~~ Sahu et al.
332 (2009) suggested that the majority of SO_4^{2-} aerosols was formed by in less than around
333 1.5 days after the air masses leftave the Chinese continent (Sahu et al., 2009). The
334 positive correlation of SO_4^{2-} and CO suggests that the secondary formation of SO_4^{2-}
335 through transport was significant during the observation period, ~~and that SO_4^{2-}~~
336 ~~contributed to the coating of BC containing particles.~~ ~~A previous study suggested~~
337 ~~that the majority of SO_4^{2-} aerosol was formed by less than around 1.5 days after the air~~

338 ~~masses left the Chinese continent (Sahu et al., 2009).~~ Kanaya et al. (2016) showed
339 that the typical transport time of continental outflow air masses at Fukue Island was
340 around 1–2 days in spring. ~~The small variability of SO₄²⁻/CO ratios is consistent~~
341 ~~with these facts.~~ The structure and composition of submicron aerosols in East Asian
342 outflow have been analyzed by using a secondary ion mass spectrometer in a
343 previous study (Takami et al., 2013). These findings suggest that SO₄²⁻ and
344 organics compose constituents in the coating of almost all of BC-containing
345 particles. Hence we hence have concluded that the formation of SO₄²⁻ during
346 transport can contribute to the growth of BC-containing particles.– The period with
347 the APT > 3 mm is highlighted by light blue in **Figure 5** to show the impacts of wet
348 removal on the transport of BC and SO₄²⁻ aerosols. The maximum concentrations of
349 BC, SO₄²⁻, and CO were observed on the morning of March 22 (Ep. 1) under the
350 influence of the anticyclone (corresponding to the trajectories colored red in **Fig. 4a**)
351 when the APT values were almost zero. In contrast, BC and SO₄²⁻ concentrations did
352 not increase with CO in the period from the evening of April 5 to the morning of April
353 6 (Ep. 2) under the influence of the migratory cyclone (corresponding to the
354 trajectories colored black in **Fig. 4a**), when the APT was greater than 10 mm.

355

356 **3.3. Correlation of BC, SO₄²⁻, and CO as an indicator of the removal of aerosols**

357 **Figures 6a** and **6b** show scatter plots of CO with BC and SO₄²⁻, respectively.
358 Positive correlation of BC and SO₄²⁻ with CO was clearly found in air masses with low
359 APT values. It is evident from these scatter plots that the ~~correlations relative~~
360 ~~enhancements~~ of BC/CO and SO₄²⁻/CO ~~are were~~ mainly ~~affected reduced~~ by the
361 APT. The cloud processes of aerosol particles not associated with precipitation can

362 also reduce the slope of their correlation. However, no decreasing tendency of
363 BC/CO and $\text{SO}_4^{2-}/\text{CO}$ slopes against RH_{max} when APT was zero was found during the
364 observation period (data not shown). Kanaya et al. (2016) found that the estimated
365 emission ratios of BC to CO over the East Asian continent ranged from 5.3 (± 2.1) to
366 6.9 (± 1.2) $\text{ng m}^{-3} \text{ppb}^{-1}$; and slightly depending depended on the origin of the air
367 masses (this range is overlaid on **Fig. 6a**). $\Delta\text{BC}/\Delta\text{CO}$ observed in the PBL over the
368 Yellow Sea ~~in during~~ the same season was 6.2 $\text{ng m}^{-3} \text{ppb}^{-1}$ (Kondo et al., 2016). The
369 data points with $\Delta\text{BC}/\Delta\text{CO}$ in these ranges show displayed low APT values (less than
370 or ~ 1 mm). Wet removal (rainout) was one of the most important controlling factors
371 on the transport efficiency of BC in this region during the observation period. This
372 work demonstrates that ~~The~~ use of ~~the~~ $\Delta\text{BC}/\Delta\text{CO}$ ratios is feasible for examining the
373 wet removal of BC during the observation period.

374 ~~The $\text{SO}_4^{2-}/\text{CO}$ slope slightly increased with RH_{max} increasing when the APT was~~
375 ~~zero, as indicated in the subset of **Figure 6b**, suggesting that aqueous phase formation~~
376 ~~and subsequent droplet evaporation partly contributed to the mass concentrations of~~
377 ~~SO_4^{2-} observed at Fukue Island. Therefore, the changes in the $\text{SO}_4^{2-}/\text{CO}$ correlation~~
378 ~~are controlled largely by the rainout process and weakly by aqueous phase formation~~
379 ~~during transport.~~ In this study, the other removal processes including dry deposition and
380 washout were considered to be minor. The dry deposition in this region has been
381 evaluated by Kanaya et al. (2016). The removal through the washout process is
382 dependent on the precipitation intensity and rain drop size as well as the particle size
383 range. We quantitatively considered the relative importance of rainout to washout.
384 The removal timescale of submicron accumulation particles through the washout was
385 estimated to be around a week or longer, which is much longer than the typical

386 transport time of air masses exported from the East Asian continent. ~~The more~~
387 details of about the estimation are given in the S.I. Note that the Aitken and coarse
388 mode particles, which were not measured by the SP2, can be significantly affected.
389 ~~The more details of the estimation are given in S.I.~~

390 The $\text{SO}_4^{2-}/\text{CO}$ slopes with the APT values of zero (i.e., non-precipitation) were
391 analyzed as a function of RH_{max} (Figure 6b). The $\text{SO}_4^{2-}/\text{CO}$ slopes without
392 precipitation varied from 30.7 to 44.1 $\text{ng m}^{-3} \text{ppb}^{-1}$ under the conditions between
393 without ($\text{RH}_{\text{max}} \geq 50\%$) and without ($\text{RH}_{\text{max}} \leq 80\%$) cloud impacts, respectively.
394 The $\text{SO}_4^{2-}/\text{CO}$ slope increased with increases in RH_{max} increasing when the APT was
395 zero, thus suggesting that—aqueous phase formation and subsequent droplet
396 evaporation partly contributed to the mass concentrations of SO_4^{2-} observed at Fukue
397 Island. Therefore, the changes in the $\text{SO}_4^{2-}/\text{CO}$ correlation were controlled largely
398 by the rainout process and weakly by aqueous-phase formation during transport.

書式変更: 上付き

書式変更: 上付き

400 **3.4. Changes in microphysical parameters of BC-containing particles associated** 401 **with wet removal**

402 Number- and mass-size distributions of BC classified by the values of $\Delta\text{BC}/\Delta\text{CO}$
403 are shown in **Figures 7a** and **7b**, respectively. When $\Delta\text{BC}/\Delta\text{CO}$ values in continental
404 outflow air masses weare greater than 3 $\text{ng m}^{-3} \text{ppb}^{-1}$ (within the range of the BC/CO
405 emission ratios given by Kanaya et al. 2016), these air masses are defined as “outflow
406 without BC loss”. These air masses originated mainly from CN via KR and NE.
407 When $\Delta\text{BC}/\Delta\text{CO}$ values of continental outflow air masses are less than 1 $\text{ng m}^{-3} \text{ppb}^{-1}$,
408 the air masses weare defined as “outflow with BC loss”. Considering the typical
409 emission ratios of BC to CO (6–7 $\text{ng m}^{-3} \text{ppb}^{-1}$; Kanaya et al., 2016), transport
410 efficiency for the “outflow with BC loss” air masses can be estimated to be less than

411 ~17%. These air masses originated mainly in CS. The low and high APT values for
412 “outflow without BC loss” and “outflow with BC loss” air masses, respectively, give
413 gave us confidence in the validity of our classification as discussed in the previous
414 section. As a reference for emission sources (“source”), the average size distributions
415 of BC in a Japanese industrial area (see section 2.1, Miyakawa et al., 2016) are shown
416 in **Figure 7**. The statistics of the size distributions awere summarized in **Table 1**.
417 Observed differences in the size distributions between source and outflow were
418 generally consistent with previous studies (Schwarz et al., 2010). Air mass aging
419 leads to the growth of BC-containing particles. Number-size distributions of BC
420 largely varied in the size range less than 0.1 μm (**Fig. 7a**). In outflow air masses,
421 such small BC-containing particles were scavenged by larger particles in the
422 coagulation process during transport. The washout process can also affect the
423 BC-containing particles in the smaller size range (<0.1 μm) as indicated in the S.I.
424 The peak diameter of mass (number) size distributions of BC became larger, i.e., from
425 0.16 (0.06) μm to 0.18–0.2 (0.09–0.1) μm , between source and outflow. The
426 BC-containing particles have had systematically different size distributions in outflow
427 air masses with and without BC loss, thus indicating that the BC loss process also
428 affected the size distributions. The peak diameter of BC number and mass size
429 distributions in outflow air masses with BC loss was slightly lower than that for air
430 masses without BC loss. The changes in the peak diameter as a function of
431 $\Delta\text{BC}/\Delta\text{CO}$ values are shown in **Figure 7c**. The observed changes in the diameter or
432 mass per particle ~~awere~~ ~~more~~ ~~very~~ ~~clearly~~ ~~found~~ and ~~awere~~ beyond the uncertainties.

433 **Figure 8** depicts the probability density of the D_S/D_{core} ratio for the BC size of 0.2
434 (± 0.02) μm ; for source and outflow air masses. The modal values of the D_S/D_{core}

書式変更: フォント : 太字

435 ratio were systematically changed with air mass aging and BC loss (wet removal).
436 The condensation of inorganic and organic vapors on BC-containing particles during
437 transport can account for the increase in the D_S/D_{core} ratio, as discussed in previous
438 studies (e.g., [Shiraiwa et al., 2008](#); Subramanian et al. 2010; ~~Shiraiwa et al., 2008~~).
439 As discussed earlier, ~~the results of~~ this study suggested that SO_4^{2-} ~~substantially~~
440 contributed substantially to the increase in the D_S/D_{core} ratio. In outflow air masses
441 with BC loss, modal values of the D_S/D_{core} ratio were clearly lower than those in
442 outflow without BC loss. ~~Furthermore, it is~~ indicated that the wet removal process
443 also affected the coating thickness distributions for the BC sizes in the range 0.15–
444 0.35 μm (**Table 1**). It should be noted that the coating of BC-containing particles is
445 not always thick in remote regions, and that the D_S/D_{core} ratio distributions, as well as
446 size distributions, can be affected by the wet removal process during transport in the
447 PBL.

448

449 **3.5. Discussion**

450 Not only in-cloud scavenging of BC-containing particles but also subsequent
451 precipitation (i.e., the rainout process) can account for the changes in the
452 microphysical parameters of BC detected in this study. Our results showed ~~the a~~
453 decrease of both the peak diameter of the BC mass size distribution, and the modal
454 value of the D_S/D_{core} ratios in relation to the rainout. The observed evidence implies
455 ~~the that there is~~ selective removal of large and water -soluble BC-containing particles
456 during transport in the PBL. The Köhler theory suggests that a lower super saturation
457 is needed for the large and highly water -soluble particles, soluble particles, and this can
458 qualitatively accounts for the observed changes in the BC microphysics. -

459 Note that the magnitude of the change in the BC size distributions in the PBL (0.01–
460 –0.02 μm (~ 1 fg)) shown in this study is smaller than that observed in air masses
461 uplifted from the PBL to the FT, ~~in association~~ with wet removal (~ 0.04 μm (~ 3 fg),
462 Fig 2 of Moteki et al., 2012) at a similar level of transport efficiency ($< \sim 20\%$). The
463 deployment of a highly sensitive instrument, SP2, enabled us to quantify such small
464 changes in the BC microphysics in the PBL. Air masses sampled at the ground level
465 would be affected by turbulent mixing of those near the clouds around the top of the
466 PBL and those in cloud-free conditions at below-cloud levels. On the other hands,
467 most air masses sampled by ~~the~~ aircraft measurements in the FT would experience the
468 cloud processes during upward transport from the PBL. Mixing of air masses in the
469 PBL suggests ~~that they~~ partially experience ~~of the~~ in-cloud scavenging processes
470 and therefore the suppression of ~~the~~ changes in the microphysical properties of
471 BC-containing particles during transport in the PBL.

472 The transport pathways of the continental outflow air masses are horizontally and
473 vertically variable in spring in East Asia because of the frequent ~~alternate~~
474 cyclone/anticyclone activities in spring (Asai et al., 1988). Oshima et al. (2013) ~~have~~
475 examined the three-dimensional transport pathways of BC over East Asia in spring and
476 showed that the PBL outflow through which BC originating from China was advected
477 by the low-level westerlies without uplifting out of the PBL was one of the ~~most~~ major
478 pathways for BC export from continental East Asia to the Pacific, thus supporting the
479 general features of microphysical properties of BC in continental outflow obtained by
480 this study. Mori et al. (2014) measured the seasonal variations in BC wet deposition
481 fluxes at another remote island in Japan (Okinawa, ~ 500 km south of Fukue Island),
482 and revealed their maxima in spring, which ~~is~~ were consistent with the seasonal

483 variations in the cyclone frequencies. It ~~is~~ has been suggested that BC-containing
484 particles were efficiently activated to form cloud droplets in the continental outflow air
485 masses, especially from the CS region, and can affect the cloud physicochemical
486 properties in spring in East Asia, as indicated by Koike et al. (2012). As the results
487 from this study are based on the observations during the limited length of the
488 periodsime, it would be worthwhile is needed to further investigate the possible
489 connections of the variabilities in BC microphysical properties and meteorological
490 conditions in this region for to providing useful constraints on more accurate
491 evaluations of climatic impacts of BC-containing particles (Matsui, 2016). To further
492 understand the possible connections of the variabilities in BC microphysical properties
493 and meteorological conditions in this region can provide useful constraints on the
494 better prediction of climatic impacts of BC containing particles (Matsui, 2016).

495

496 4. Conclusions

497 Ground-based measurements of BC were performed near an industrial source region
498 and at a remote island in Japan. We have reported on the temporal variations in the
499 transport and the microphysics of the BC-containing particles that were, measured by
500 using ~~the~~ COSMOS, SP2, and ACSM. The impacts of air mass aging upon the
501 growth of BC-containing particles were examined by comparing the ground-based
502 observations between the near-source and remote island sites. $\Delta BC/\Delta CO$ was used as
503 an indicator of the transport efficiency of BC, because it was controlled mainly by
504 rainout during transport in the PBL. The BC size and coating increased during
505 transport from the near-source to the outflow regions on the timescale of 1–2 days
506 when the rainout during transport was negligible. SO_4^{2-} aerosol was secondarily

507 formed both in the gas- and cloud-phases during transport, and it contributed to the
508 significant increase in the coating materials of BC (i.e., it enhanced the whole size and
509 water-solubility of BC-containing particles). Decreases in the peak diameter of mass
510 size distributions ($\sim 0.01 \mu\text{m}$) and modal D_g/D_{core} ratios (~ 0.4 for BC with a diameter of
511 $0.2 \mu\text{m}$) of BC-containing particles were observed in air masses substantially affected
512 by rainout. The observed evidences, for the selective removal of large and
513 water-soluble BC-containing particles, was are qualitatively consistent with the Köhler
514 theory; however the they values are-were not as large as those found in air masses
515 uplifted from the PBL to the FT in East Asia associated with precipitation. The
516 mixing of below-cloud and in-cloud air masses in the PBL would result in suppression
517 of the degree of changes in BC microphysical parameters by cloud processes. This
518 study indicates (1) that the changes (sign and degree) in BC microphysics can be
519 affected by how the air masses are transported and; (2) that the observed selective
520 removal of large and water-soluble BC-containing particles in East Asia are-can be
521 expected to be significant in the PBL as well as in the FT in East Asia.

522

523

524 **Acknowledgments**

525 This study was supported by the Environment Research and Technology
526 Development Fund (S7, S12, and 2-1403) of the Ministry of Environment, Japan, and
527 the Japan Society for the Promotion of Science (JSPS), KAKENHI Grant numbers
528 JP26550021, JP26701004, JP26241003, JP16H01772, and JP16H01770, and the
529 research was partially carried out in the Arctic Challenge for Sustainability (ArCS)
530 Project. The authors would like to thank N. Moteki and S. Ohata at the University of

531 Tokyo for assistance with the SP2 calibrations. M. Kubo, T. Takamura, and H. Irie
532 (Chiba University) are also acknowledged for their support at the Fukue-Island
533 Atmospheric Environment Monitoring Station.

534

535 **References**

536 Asai, T., Y. Kodama, and J.-C. Zhu, Long-term variations of cyclone activities in East
537 Asia, *Adv. Atmos. Sci.*, 5, 149–158, 1988.

538 Bond, T. C. and R. W. Bergstrom, Light Absorption by Carbonaceous Particles: An
539 Investigative Review, *Aerosol Sci. Technol.*, 40, 27-67, 2006.

540 Bond, T., et al.. Bounding the role of black carbon in the climate system: a scientific
541 assessment. *J. Geophys. Res.*, 118, 5380–5552, doi:10.1002/jgrd.50171, 2013.

542 Draxler, R. R., and Rolph, G. D., HYSPLIT (HYbrid Single-Particle Lagrangian
543 Integrated Trajectory) Model access via NOAA ARL READY Website
544 (<http://ready.arl.noaa.gov/HYSPLIT.php>), NOAA Air Resources Laboratory,
545 Silver Spring, Md., 2012

546 Gao, R. S., Schwarz, J. P., Kelly, K. K., Fahey, D. W., Watts, L. A., Thompson, T. L.,
547 Spackman, J. R., Slowik, J. G., Cross, E. S., Han, J. H., Davidovits, P., Onasch, T.
548 B., and Worsnop, D. R., A novel method for estimating light-scattering properties
549 of soot aerosols using a modified single-particle soot photometer, *Aerosol Sci.*
550 *Tech.*, 41, 125–135, 2007

551 Hinds, W. C., *Aerosol Technology: Properties, Behavior, and Measurement of Airborne*
552 *Particles*, Wiley-Interscience, New York, 1999

553 Huffman, G.J., R.F. Adler, M. Morrissey, D.T. Bolvin, S. Curtis, R. Joyce, B
554 McGavock, and J. Susskind, *Global Precipitation at One-Degree Daily Resolution*

555 from Multi-Satellite Observations. *J. Hydrometeor.*, 2, 36-50, 2001

556 Ikeda, K., K. Yamaji, Y. Kanaya, F. Taketani, X. Pan, Y. Komazaki, J. Kurokawa, and T.
557 Ohara, Sensitivity Analysis of Source Regions to PM_{2.5} Concentration at Fukue
558 Island, Japan, *J. Air Waste Manage. Assoc.*, doi:10.1080/10962247.2013.845618,
559 2014

560 Irei, S., A. Takami, M. Hayashi, Y. Sadanaga, K. Hara, N. Kaneyasu, K. Sato, T.
561 Arakaki, S. Hatakeyama, H. Bandow, T. Hikida, and A. Shimono, Transboundary
562 Secondary Organic Aerosol in Western Japan Indicated by the $\delta^{13}\text{C}$ of
563 Water-Soluble Organic Carbon and the m/z 44 Signal in Organic Aerosol Mass
564 Spectra, *Environ. Sci. Technol.*, 48, 6273-6281, 2014

565 Kanaya, Y., F. Taketani, Y. Komazaki, X. Liu, Y. Kondo, L. K. Sahu, H. Irie, and H.
566 Takashima, Comparison of black carbon mass concentrations observed by
567 Multi-Angle Absorption Photometer (MAAP) and Continuous Soot-Monitoring
568 System (COSMOS) on Fukue Island and in Tokyo, Japan, *Aerosol Sci. Technol.*,
569 47, 1-10, 2013

570 Kanaya, Y., X. Pan, T. Miyakawa, Y. Komazaki, F. Taketani, I. Uno, and Y. Kondo,
571 Long-term observations of black carbon mass concentrations at Fukue Island,
572 western Japan, during 2009-2015: Constraining wet removal rates and emission
573 strengths from East Asia, *Atmos. Phys. Chem. Discuss.*, 16, 10689-10705,
574 doi:10.5194/acp-2016-21310689-2016, 2016.

575 Koike, M., N. Takegawa, N. Moteki, Y. Kondo, H. Nakamura, K. Kita, H. Matsui, N.
576 Oshima, M. Kajino, and T. Y. Nakajima, Measurements of regional-scale aerosol
577 impacts on cloud microphysics over the East China Sea: Possible influences of
578 warm sea surface temperature over the Kuroshio ocean current, *J. Geophys. Res.*,

579 117, D17205, doi:10.1029/2011JD017324, 2012

580 Kondo, Y., L. Sahu, N. Moteki, F. Khan, N. Takegawa, X. Liu, M. Koike and T.
581 Miyakawa, Consistency and Traceability of Black Carbon Measurements Made by
582 Laser-Induced Incandescence, Thermal-Optical Transmittance, and Filter-Based
583 Photo-Absorption Techniques, *Aerosol Sci. Technol.*, 45, 295-312, 2009

584 Kondo, Y., N. Moteki, N. Oshima, S. Ohata, M. Koike, Y. Shibano, N. Takegawa,
585 and K. Kita, Effects of Wet Deposition on the Abundance and Size Distribution of
586 Black Carbon in East Asia, *J. Geophys. Res. Atmos.*, 121,
587 doi:10.1002/2015JD024479, 2016

588 Kurokawa, J., T. Ohara, T. Morikawa, S. Hanayama, G. Janssens-Maenhout, T. Fukui,
589 K. Kawashima, and H. Akimoto, Emissions of air pollutants and greenhouse gases
590 over Asian regions during 2000-2008: Regional Emission inventory in ASia
591 (REAS) version 2, *Atmos. Chem. Phys.*, 13, 11019-11058,
592 doi:10.5194/acp-13-11019-2013, 2013

593 Kuwata, M., Y. Kondo, M. Mochida, N. Takegawa, and K. Kawamura, Dependence of
594 CCN activity of less volatile particles on the amount of coating observed in Tokyo,
595 *J. Geophys. Res.*, 112, D11207, doi:10.1029/2006JD007758, 2007

596 Kuwata, M., Y. Kondo, and N. Takegawa, Critical condensed mass for activation of
597 black carbon as cloud condensation nuclei in Tokyo, *J. Geophys. Res.*, 114,
598 D20202, doi:10.1029/2009JD012086, 2009

599 Laborde, M., Mertes, P., Zieger, P., Dommen, J., Baltensperger, U., and Gysel, M.,
600 Sensitivity of the Single Particle Soot Photometer to different black carbon types,
601 *Atmos. Meas. Tech.*, 5, 1031–1043, doi:10.5194/amt-5-1031-2012, 2012

602 Lawrence, M., T. M. Butler, J. Steinkamp, B. R. Gurjar, and J. Lelieveld, Regional

603 pollution potentials of megacities and other major population centers, *Atmos.*
604 *Chem. Phys.*, 7, 3969-3987, 2007

605 Liu, J., S. Fan, L. W. Horowitz, and H. Levy II, Evaluation of factors controlling
606 long-range transport of black carbon to the Arctic, *J. Geophys. Res.*, 116, D04307,
607 doi:10.1029/2010JD015145, 2011

608 Mari, X., et al., Effects of soot deposition on particle dynamics and microbial
609 processes in marine surface waters, *Global Biogeochem. Cycles*, 28, 662–678,
610 doi:10.1002/2014GB004878, 2014

611 Matsui, H., Black carbon simulations using a size- and mixing-state-resolved
612 three-dimensional model: 1. Radiative effects and their uncertainties, *J. Geophys.*
613 *Res. Atmos.*, 121, 1793–1807, doi:10.1002/2015JD023998, 2016

614 McMeeking, G. R., N. Good, M. D. Petters, G. McFiggans, and H. Coe, Influences
615 on the fraction of hydrophobic and hydrophilic black carbon in the atmosphere,
616 *Atmos. Chem. Phys.*, 11, 5099-5112, 2011

617 Miyakawa, T., Y. Kanaya, Y. Komazaki, F. Taketani, X. Pan, M. Irwin, J. Symonds,
618 Intercomparison between a single particle soot photometer and evolved gas
619 analysis in an industrial area in Japan: Implications for the consistency of soot
620 aerosol mass concentration measurements, *Atmos. Environ.*, 127, 14-21, 2016

621 Mori, T., Y. Kondo, S. Ohata, N. Moteki, H. Matsui, N. Oshima, and A. Iwasaki, Wet
622 deposition of black carbon at a remote site in the East China Sea, *J. Geophys. Res.*
623 *Atmos.*, 119, 10,485–10,498, doi:10.1002/2014JD022103, 2014

624 [Moteki, N., and Kondo, Y.. Dependence of laser-induced incandescence on physical](#)
625 [properties of black carbon aerosols: measurements and theoretical interpretation.](#)
626 [Aerosol Sci. Technol.](#), 44, 663-675, 2011

627 Moteki, N., Y. Kondo, N. Oshima, N. Takegawa, M. Koike, K. Kita, H. Matsui, and M.
628 Kajino, Size dependence of wet removal of black carbon aerosols during transport
629 from the boundary layer to the free troposphere, *Geophys. Res. Lett.*, 39, L13802,
630 doi:10.1029/2012GL052034, 2012

631 Oshima, N., M. Koike, Y. Zhang, Y. Kondo, N. Moteki, N. Takegawa, and Y.
632 Miyazaki, Aging of black carbon in outflow from anthropogenic sources using a
633 mixing state resolved model: Model development and evaluation, *J. Geophys. Res.*,
634 114, D06210, doi:10.1029/2008JD010680, 2009

635 Oshima, N., et al., Wet removal of black carbon in Asian outflow: Aerosol Radiative
636 Forcing in East Asia (A-FORCE) aircraft campaign, *J. Geophys. Res.*, 117,
637 D03204, doi:10.1029/2011JD016552, 2012

638 Oshima, N., and M. Koike, Development of a parameterization of black carbon aging
639 for use in general circulation models, *Geophys. Model. Dev.*, 6, 263-282, 2013

640 Oshima, N., M. Koike, Y. Kondo, H. Nakamura, N. Moteki, H. Matsui, N. Takegawa,
641 and K. Kita, Vertical transport mechanisms of black carbon over East Asia in
642 spring during the A-FORCE aircraft campaign, *J. Geophys. Res. Atmos.*, 118,
643 13,175–13,198, doi:10.1002/2013JD020262, 2013

644 Petzold, A., J.A. Ogren, M., Fiebig, S. M. Li, U. Bartensperger, T. Holzer-Popp, S.
645 Kinne, G. Pappalardo, N. Sugimoto, C. Wehrli, A. Wiedensohler, and X. Y. Zhang,
646 Recommendations for reporting “black carbon” measurements, *Atmos. Chem.*
647 *Phys.* 13, 8365-8379, 2013

648 Rolph, G. D., Real-time Environmental Applications and Display system (READY)
649 Website (<http://ready.arl.noaa.gov>). NOAA Air Resources Laboratory, Silver
650 Spring, Md., 20192

651 Sahu, L. K., Y. Kondo, Y. Miyazaki, M. Kuwata, M. Koike, N. Takegawa, H.
652 Tanimoto, H. Matsueda, S. C. Yoon, and Y. J. Kim, Anthropogenic aerosols
653 observed in Asian continental outflow at Jeju Island, Korea, in spring 2005, J.
654 Geophys. Res., 114, D03301, doi:10.1029/2008JD010306, 2009

655 Samset, B. H., et al., Modelled black carbon radiative forcing and atmospheric lifetime
656 in AeroCom Phase II constrained by aircraft observations, Atmos. Phys. Chem., 14,
657 12465-12477, 2014

658 Schwarz, J. P., J. R. Spackman, R. S. Gao, L. A. Watts, P. Stier, M. Schulz, S. M.
659 Davis, S. C. Wofsy, and D. W. Fahey, Global - scale black carbon profiles
660 observed in the remote atmosphere and compared to models, Geophys. Res. Lett.,
661 37, L18812, doi:10.1029/2010GL044372, 2010

662 Seinfeld, J.H., and Pandis, S. N., Atmospheric Chemistry and Physics, 2nd ed., John
663 Wiley & Sons, New York, 2006

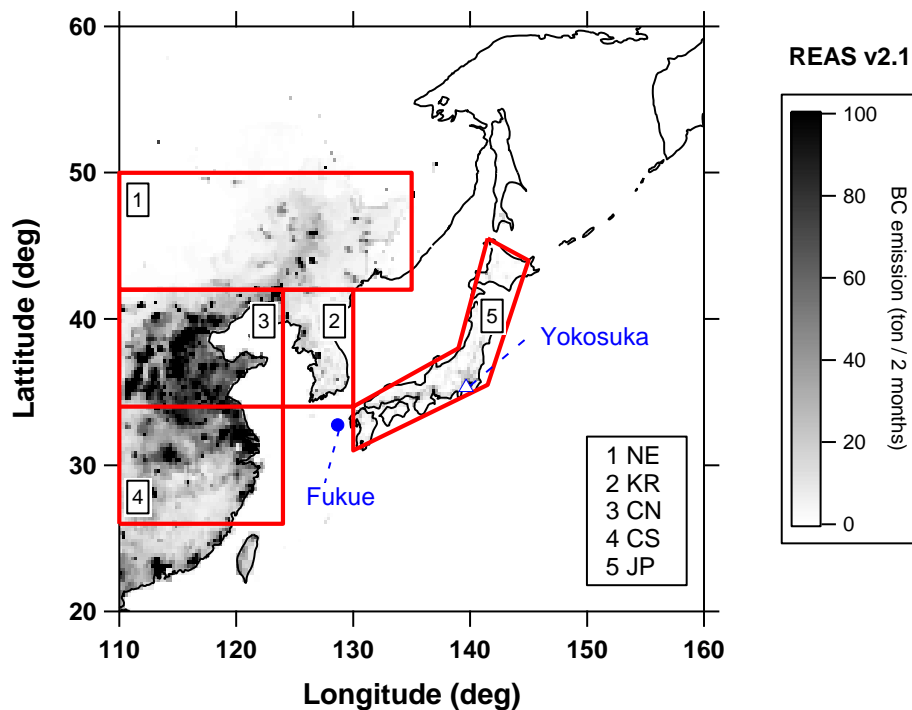
664 Shiraiwa M., Y. Kondo, N. Moteki, N. Takegawa, L. K. Sahu, A. Takami, S.
665 Hatakeyama, S. Yonemura, and D. R. Blake, Radiative impact of mixing state of
666 black carbon aerosol in Asian outflow, J. Geophys. Res. 113, D24210,
667 doi:10.1029/2008JD010546, 2008

668 Subramanian, R., G. L. Kok, D. Baumgardner, A. Clarke, Y. Shinozuka, T. L. Campos,
669 C. G. Heizer, B. B. Stephens, B. de Foy, P. B. Voss, and R. A. Zaveri, Black
670 carbon over Mexico: the effect of atmospheric transport on mixing state, mass
671 absorption cross-section, and BC/CO ratios, Atmos. Chem. Phys., 10, 219-237,
672 2010

673 Takami A., T. Miyoshi, A. Shimono, N. Kaneyasu, S. Kato, Y. Kajii, and S.
674 Hatakeyama, Transport of anthropogenic aerosols from Asia and subsequent

675 chemical transformation. J. Geophys. Res., 112 (D22S31),
676 doi:10.1029/2006JD008120, 2007
677 [Takami, A., et al., Structural analysis of aerosol particles by microscopic observation](#)
678 [using a time-of-flight secondary ion mass spectrometer, J. Geophys. Res. Atmos.,](#)
679 [118, 6726–6737, doi:10.1002/jgrd.50477, 2013](#)
680 [Yoshino, A., A. Takam, K. Sato, A. Shimizu, N. Kaneyasu, S. Hatakeyama, K. Hara,](#)
681 [and M. Hayashi. Influence of Trans-Boundary Air Pollution on the Urban](#)
682 [Atmosphere in Fukuoka, Japan. Atmosphere, 7, 51, doi:10.3390/atmos7040051,](#)
683 [2016](#)
684

685 **Figures**

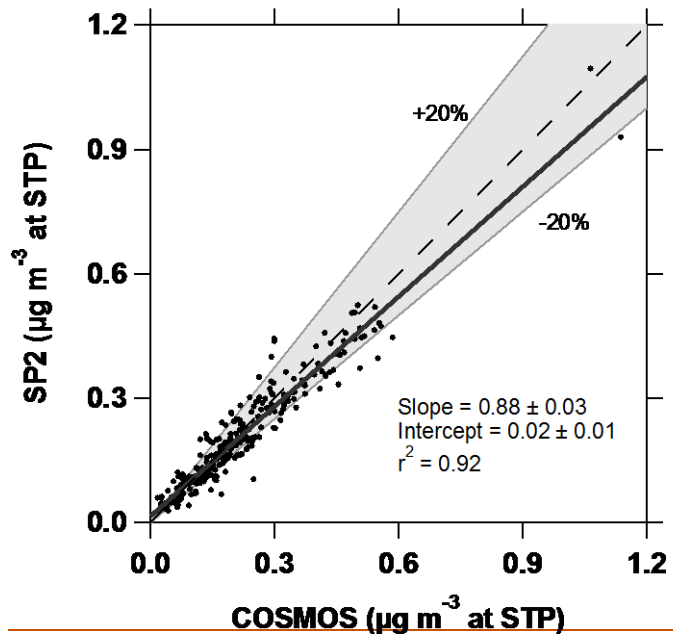


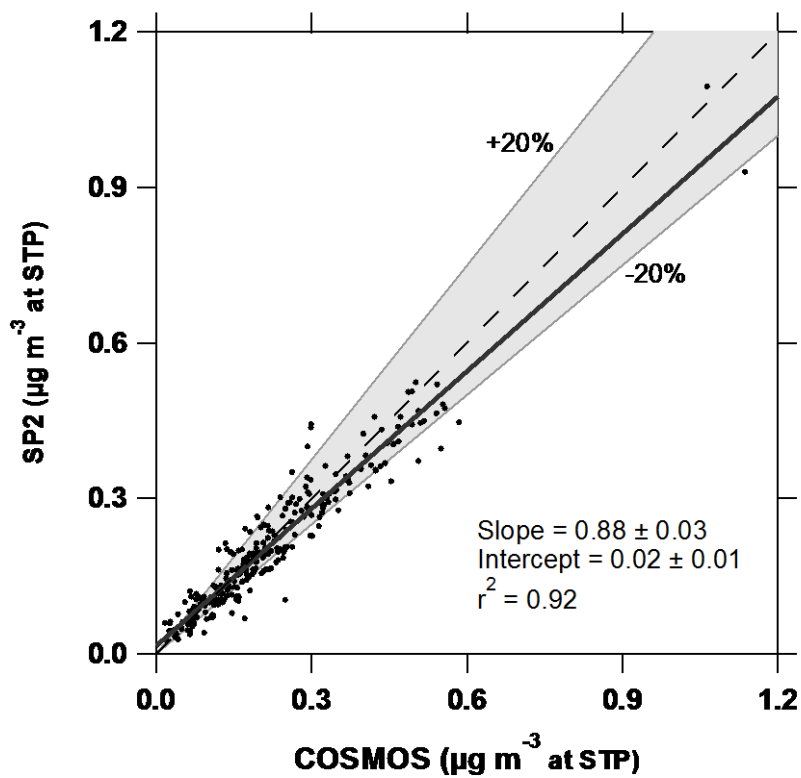
686

687

688 **Figure 1.** Map of the investigated region with two observation sites (Yokosuka, open
689 triangle; Fukue Island, closed circle) and five defined areas (1 Northeast China; 2
690 Korea; 3 Central North China; 4 Central South China; 5 Japan). The bimonthly mean
691 BC emission rate (March–April) in 2008 is overlaid on the map (REAS ver. 2.1,
692 Kurokawa et al., 2013).

693



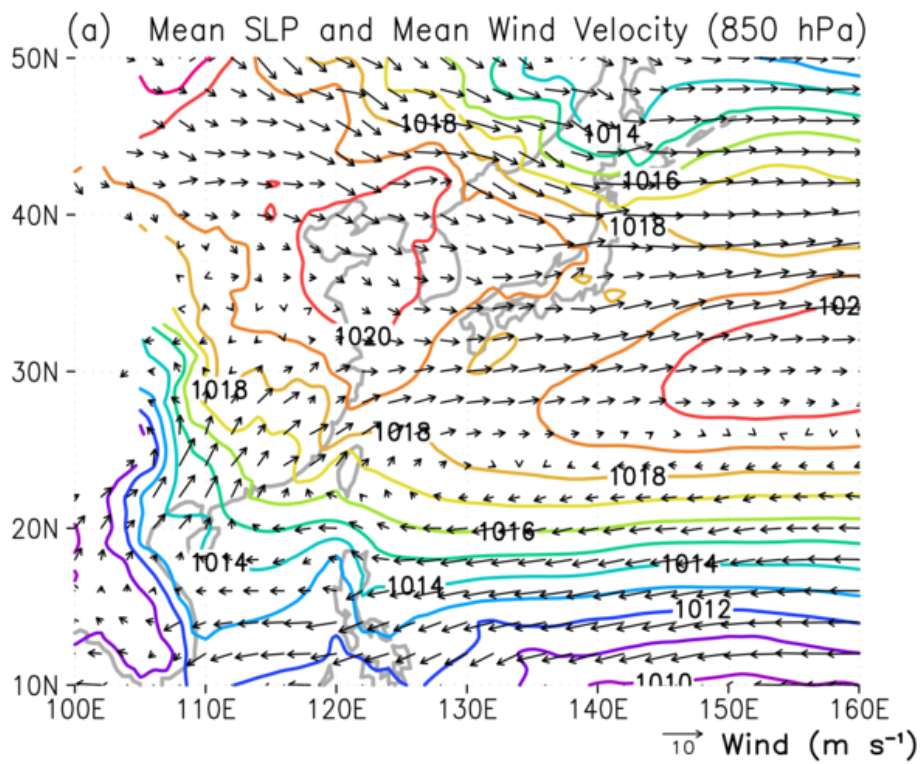


695

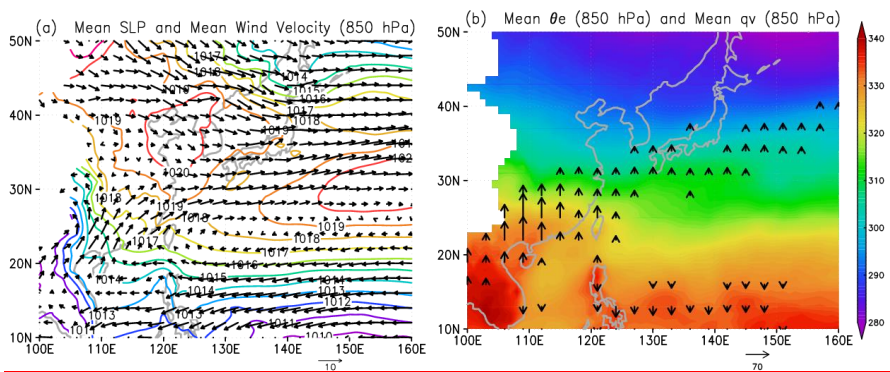
696

697 **Figure 2.** Correlation plot of SP2-rBC and COSMOS-EBC mass concentrations (at
698 standard temperature and pressureSTP). The shaded region corresponds to the levels
699 within $\pm 20\%$.

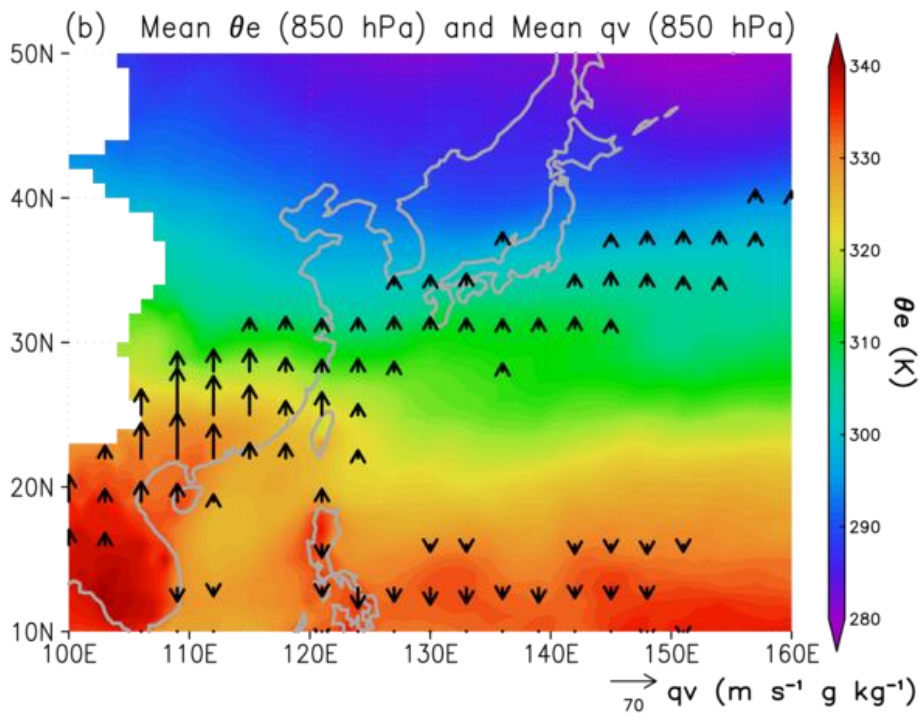
700



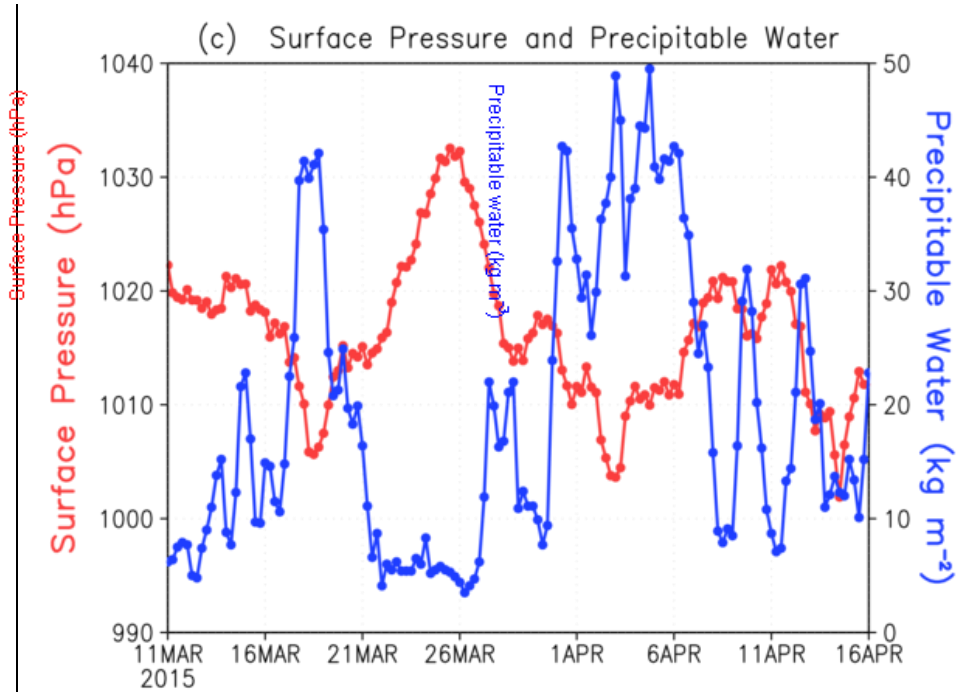
701



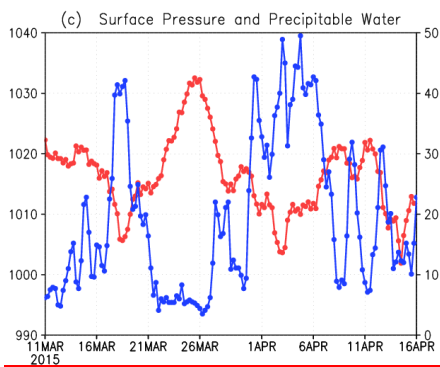
702



703



704



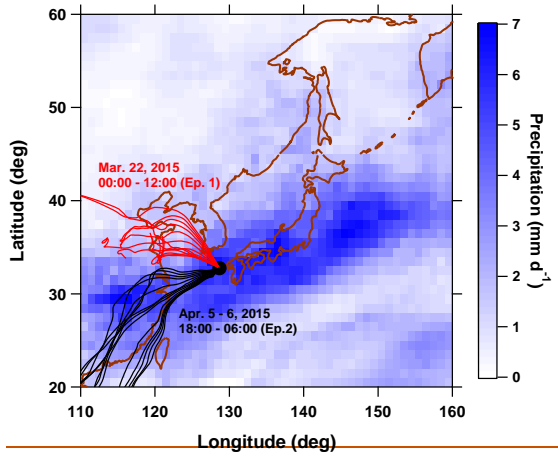
705

706

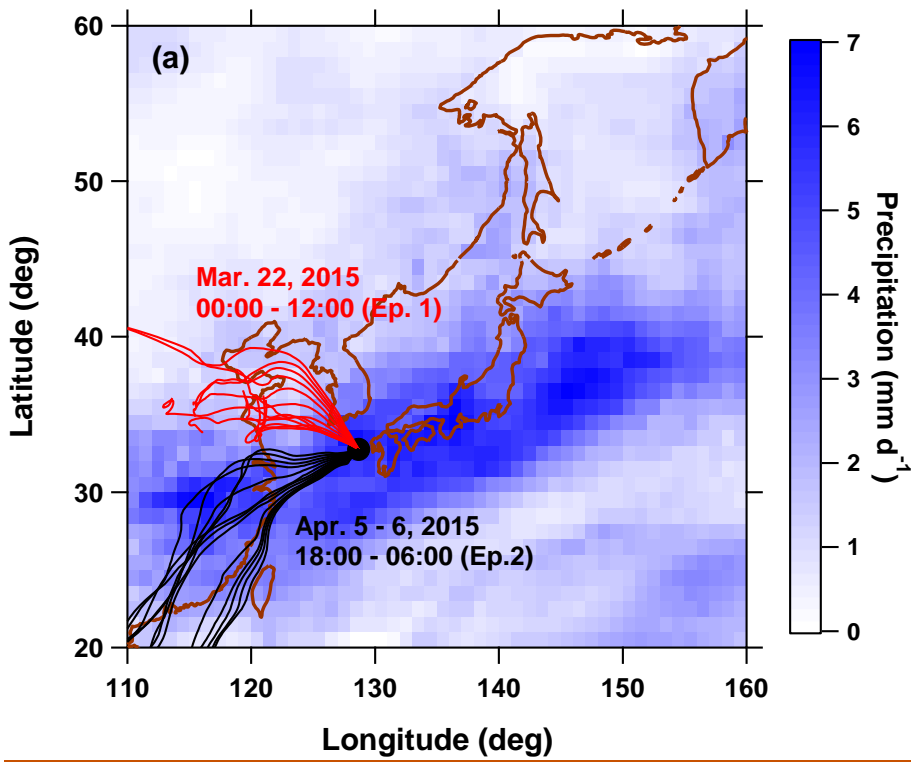
707 **Figure 3.** Meteorological fields in East Asia during the observation period (March 11–
 708 –April 14, 2015) based on NCEP FNL data. (a) Mean SLP (hPa, contours) and mean
 709 horizontal wind velocity at the 850-hPa level (m s^{-1}). Regions without data
 710 correspond to those of high-altitude mountains. (b) Mean θ_e (K) and total meridional

711 moisture transport (qv values) at the 850-hPa level ($\text{m s}^{-1} \text{g kg}^{-1}$). Only qv vectors
712 with magnitudes greater than $10 \text{ m s}^{-1} \text{g kg}^{-1}$ were plotted. (c) Temporal variations in
713 the surface pressure (hPa, red line and markers with left axis) and precipitable water
714 (kg m^{-2} , blue line and markers with right axis) at the Fukue observation site (32.75°N ,
715 128.68°E).
716

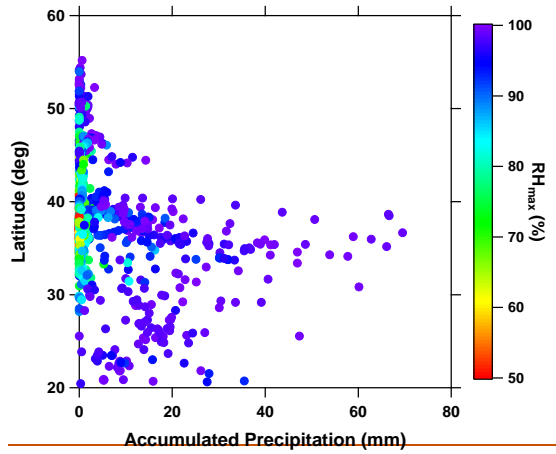
717



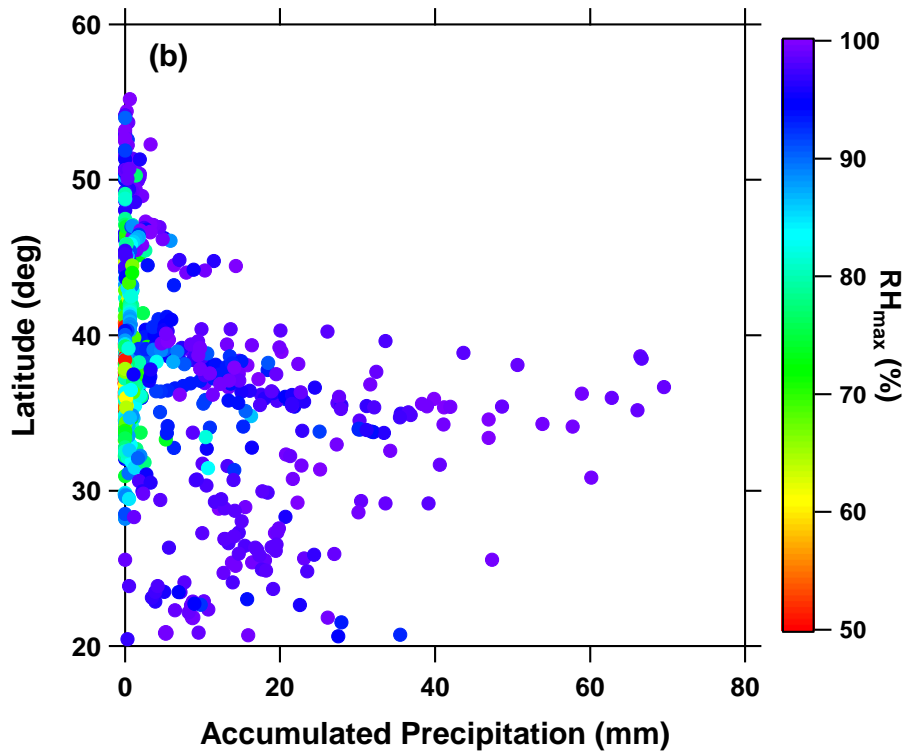
718



719



720



721

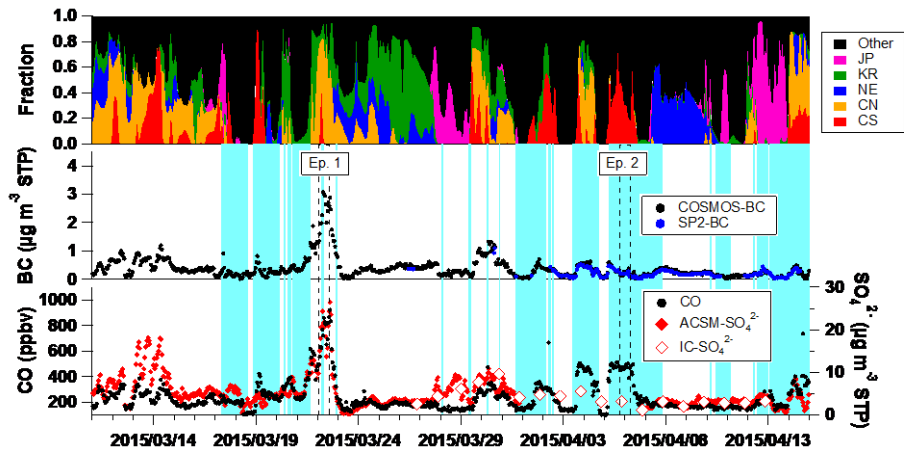
722 **Figure 4.** (a) Mean precipitation derived from GPCP during the observation period
723 (March 11–April 14, 2015). (b) Three-day backward trajectories for selected periods

724 | are overlaid (~~Red~~ lines, 00:00–12:00LT March 22, 2015 (Ep.1); ~~Black~~ lines,
725 | 08:00LT, April 5–06:00LT, April 6, 2015 (Ep.2)). (b) The relationship between APT
726 | and L_{ORIG} (see text for details) colored by the maximum RH along the backward
727 | trajectories.

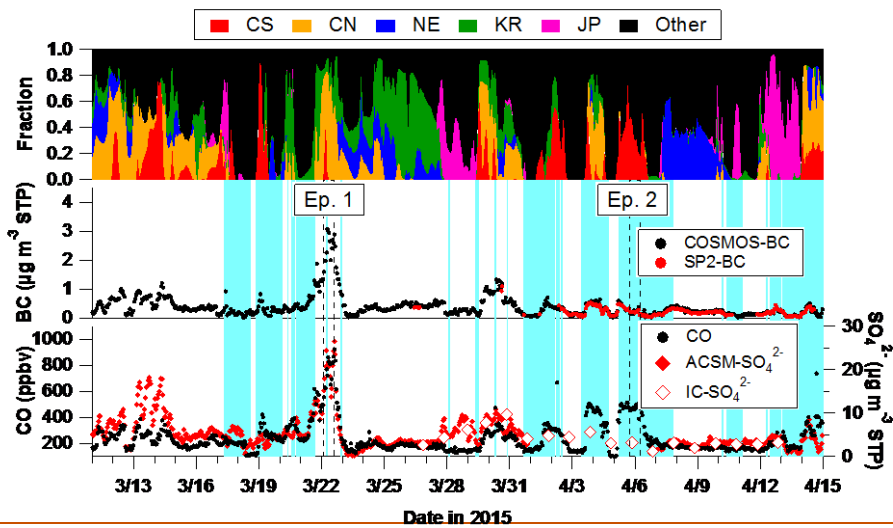
728 | _____

書式変更：両端揃え，行間：1.5行，
改ページ時1行残して段落を区切る

書式変更: 左揃え, 行間: 1行, 改ページ時1行残して段落を区切らない

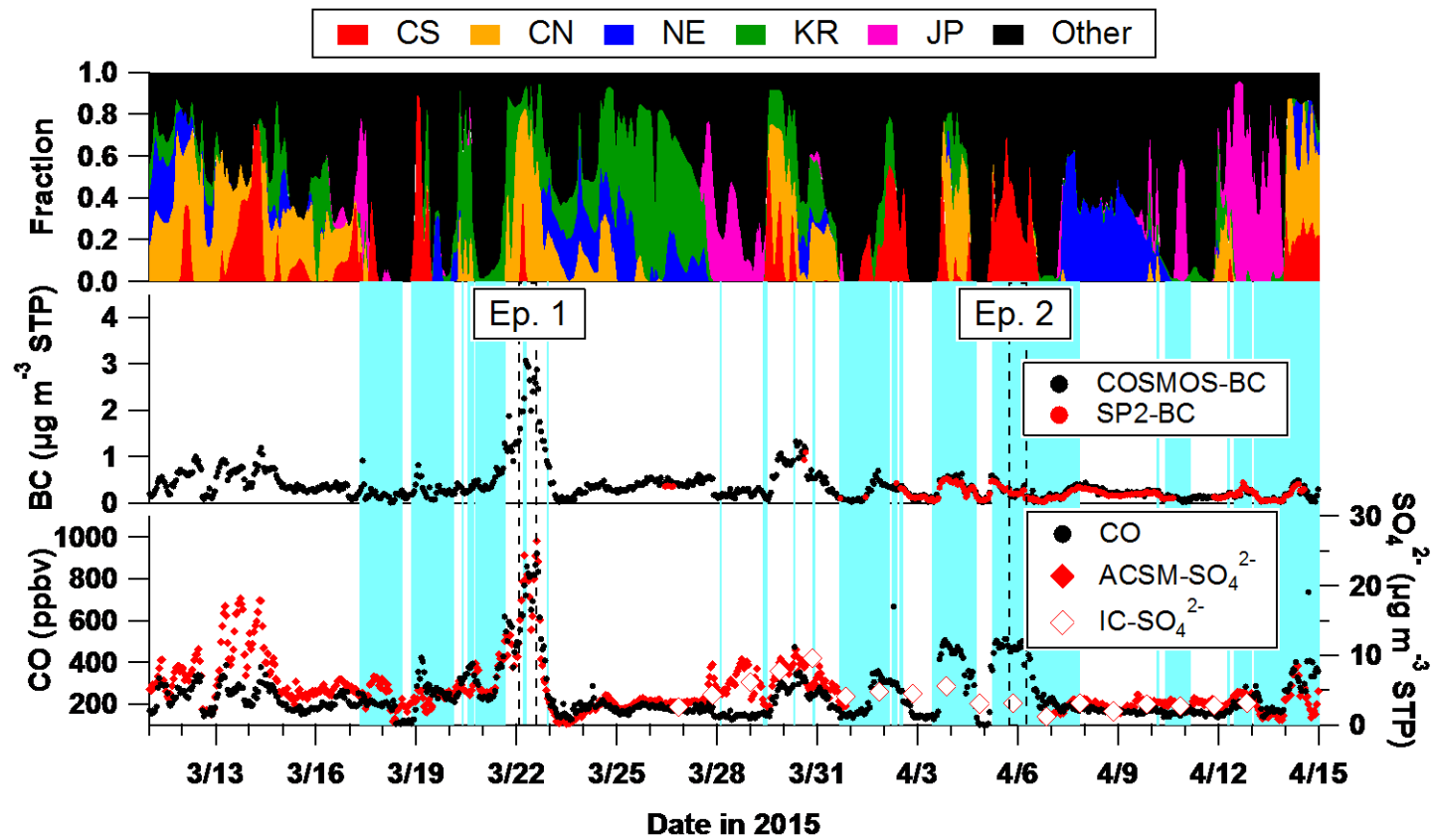


729



730

731 **Figure 5.** Temporal variations in air mass origin and concentration of trace species.—
 732 (Top panel) Fractional residence time of air masses passed over selected area (Red,
 733 Central South China; Orange, Central North China; Blue, Northeast China; Green,
 734 Korea; Pink, Japan; Black, other regions such as Ocean).—(Middle panel) mass
 735 concentrations of BC measured using the COSMOS (black markers) and SP2 (blue red
 736 markers).—(Bottom panel) concentrations of CO (black markers) and SO_4^{2-} (red
 737 circles and open diamond for ACSM and IC, respectively).—The periods with the APT
 738 > 3 mm are highlighted in light blue in the middle and bottom panels.—The periods
 739 denoted as Ep.1 and Ep.2 (see the text for details) were enclosed by dashed lines.



740

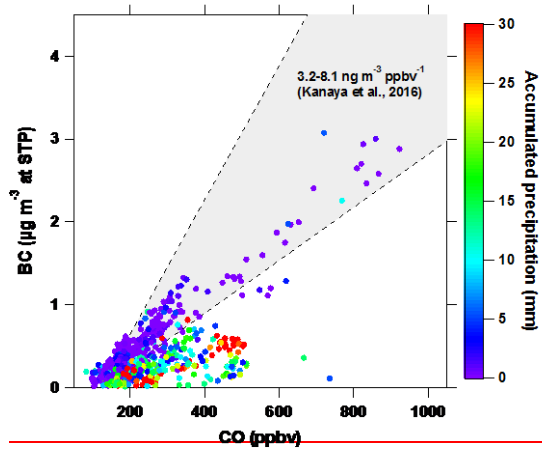
741

742

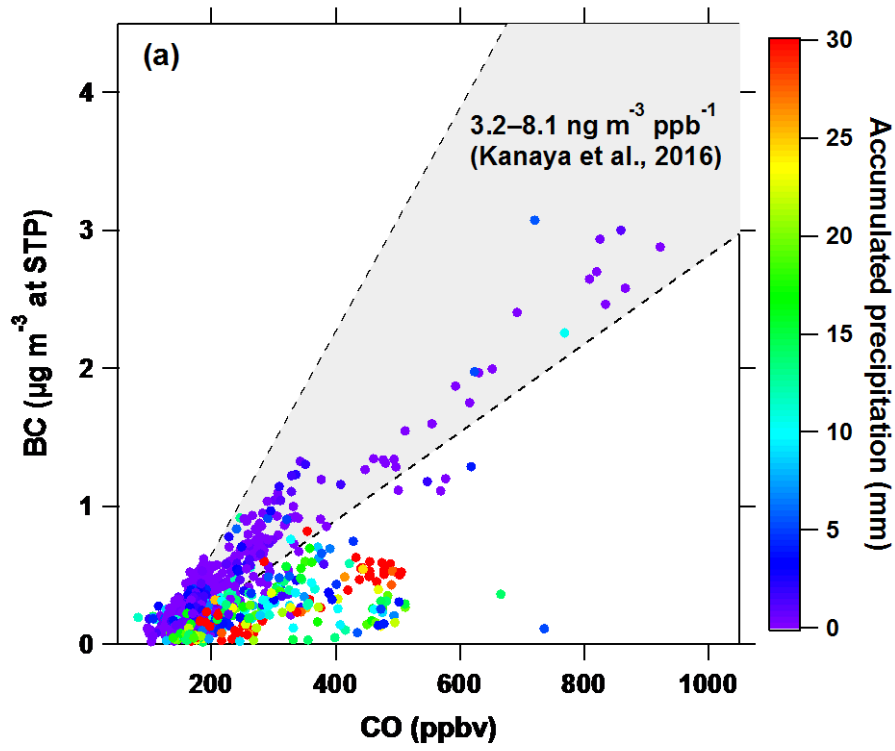
Figure 5. Temporal variations in air mass origin and concentration of trace species. (Top panel) Fractional residence time of air masses

743 | that passed over the selected area (red, Central South China; orange, Central North China; blue, Northeast China; green, Korea; pink,
744 | Japan; black, other regions such as the Ocean). (Middle panel) Mass concentrations of BC measured by using COSMOS (black
745 | markers) and SP2 (red markers). (Bottom panel) Concentrations of CO (black markers) and SO₄²⁻ (red circles and open diamonds for
746 | ACSM and IC, respectively). The periods with the APT >3 mm are highlighted in light blue in the middle and bottom panels. The
747 | periods denoted as Ep. 1 and Ep. 2 (see the text for details) were enclosed by dashed lines.

748



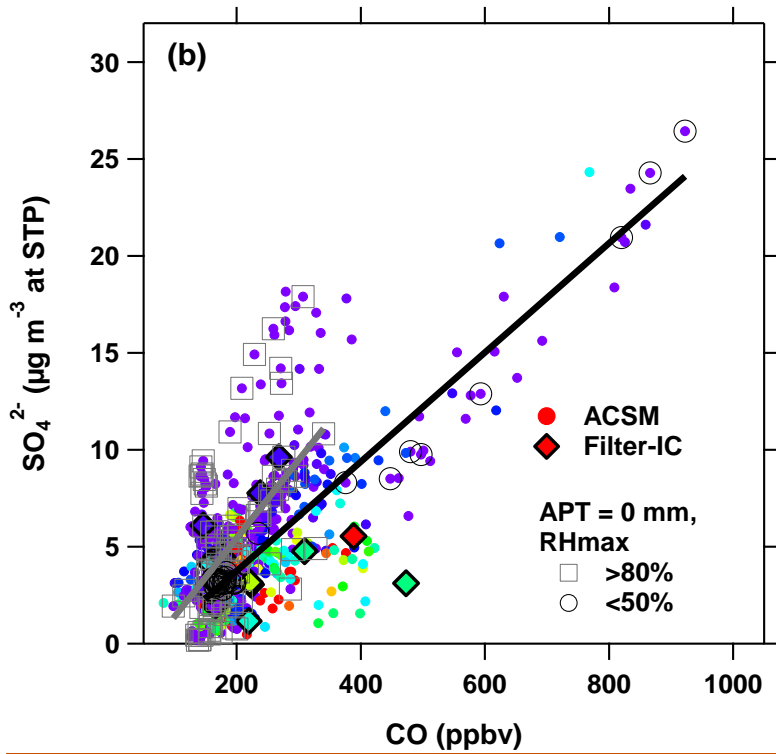
749



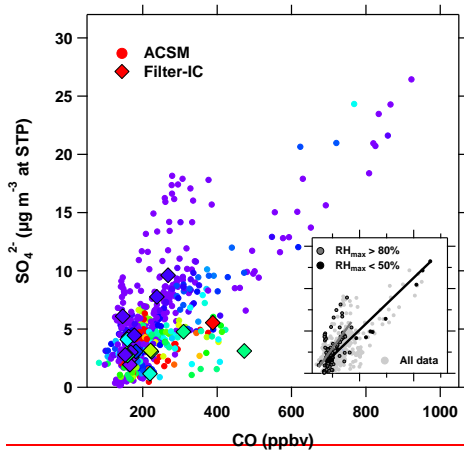
750

書式変更: 左揃え

書式変更: 標準の文字数



751



752

753

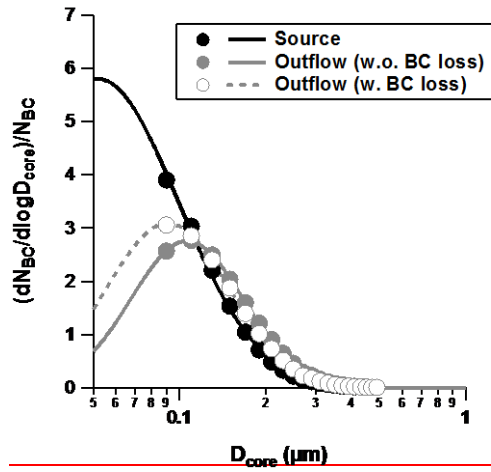
754 **Figure 6.** Correlation between aerosol mass concentrations and the CO mixing ratio
 755 colored according to the APT. (a) BC measured by COSMOS and (b) SO_4^{2-} measured
 756 by ACSM and IC (circles and diamonds s-markers, respectively). ACSM-- SO_4^{2-} /CO

書式変更: 左揃え, インデント: 最初の
行: 0 字

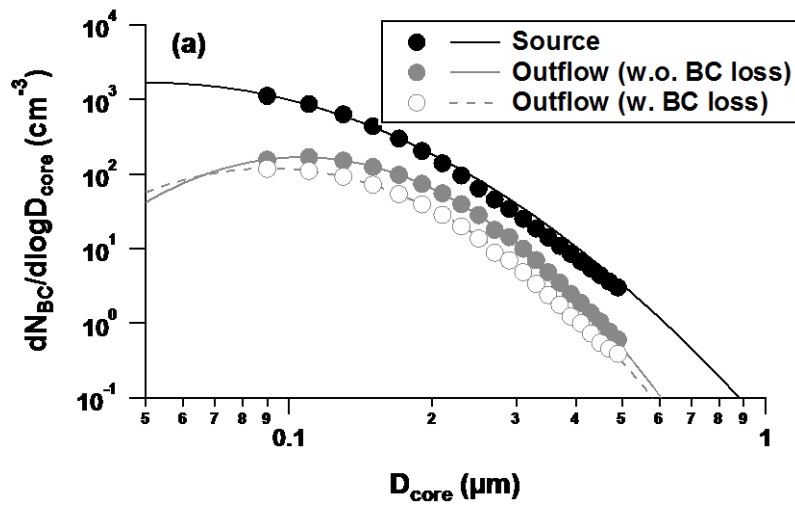
757 | correlations for the zero-APT air masses (no precipitation during transport) with
758 | ~~symbols indicating if the RH_{max} greater than above 80% (dark shaded cross open~~
759 | ~~squares markers) or less than below 50% (black open circles crosses) are in the subset of~~
760 | ~~6 overlaid.~~
761

書式変更: 下付き

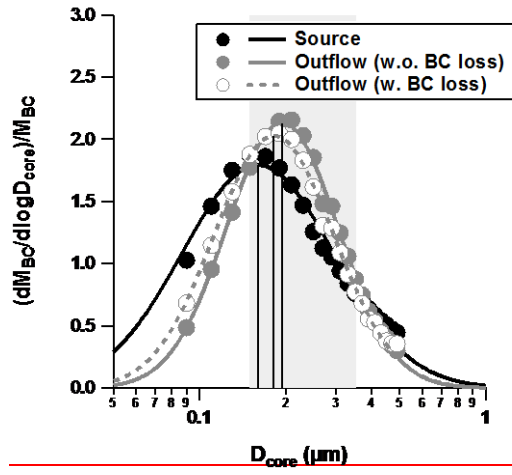
762



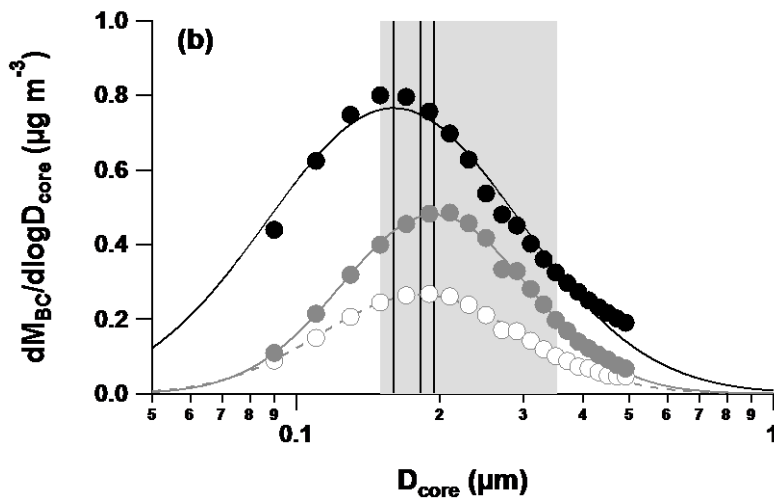
763

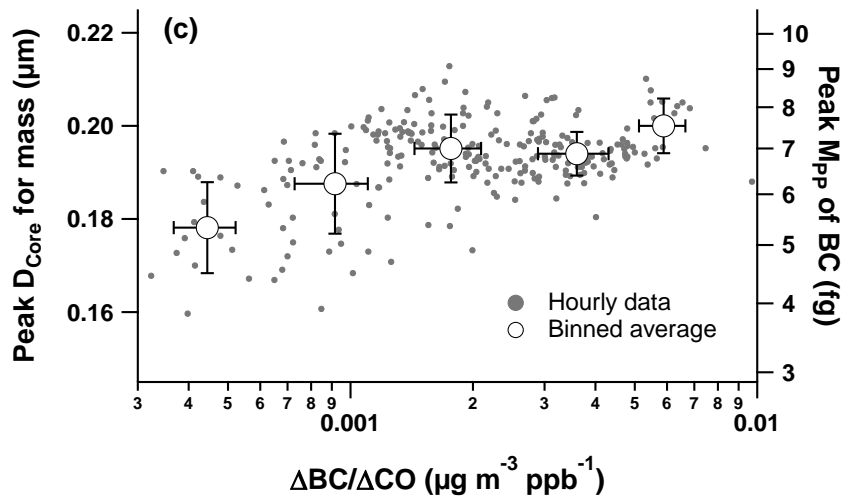


764



765





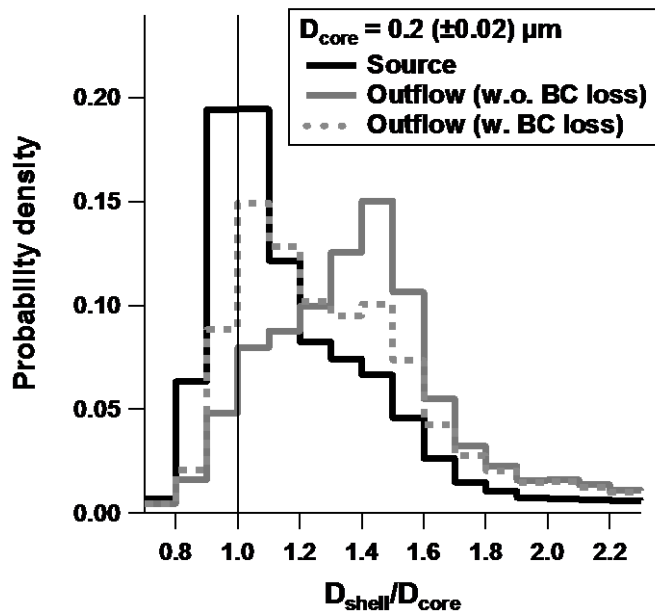
766

767

768 **Figure 7.** The (a) number and (b) mass size distributions of BC measured at Yokosuka
 769 (black markers) and at Fukue Island (gray markers). (c) The evolution of the peak
 770 D_{core} as a function of the degree of removal of BC (i.e., $\Delta\text{BC}/\Delta\text{CO}$ ratios).—All the size
 771 distributions are normalized by the number or mass concentrations of BC integrated for
 772 the diameter range of 0.08–0.5 μm . The size distributions at Fukue Island include the
 773 data for the outflow air masses with (open markers) and without (closed markers) BC
 774 loss. Lines are the lognormal fitting results. The shaded band in 6(b) corresponds to
 775 the size range analyzed to estimate D_s/D_{core} ratios. Vertical lines in 6(b) represent the
 776 peak diameter of the lognormal fit for each of three mass size distributions. Note that
 777 the peak diameter of the Loglog-normal fit for the BC number size distributions at
 778 Yokosuka was estimated from the peak diameter of its mass size distribution (**Table 1**).

書式変更: フォント: 斜体

書式変更: 下付き



779

780

781 **Figure 8.** Probability density function of the estimated D_s/D_{core} ratios for BC-containing
 782 particles with the size $0.2 (\pm 0.02) \mu m$ at Yokosuka (~~Black-black~~ line) and in the air
 783 masses of continental outflow with (gray dashed line) and without (gray solid line) BC
 784 loss.

785

786
787
788

Tables

Table 1. Summaries of BC microphysical parameters measured at Yokosuka and Fukue Island

789

790

791

Site	Air mass type	Averaging time* (hrs)	$\Delta BC/\Delta CO$ ($\text{ng m}^{-3} \text{ppb}^{-1}$)	APT (mm)	Log Normal Fit Parameters Avg. (1σ)		1-hr Median D_s/D_{core} for selected D_{core} Avg. (1σ)			
					MMD (μm)	σ_g	0.15 - 0.2	0.2 - 0.25	0.25 - 0.3	0.3 - 0.35 (μm)
Yokosuka	Source	184	-	-	0.160 (0.019)	1.84 (0.08)	1.18 (0.07)	1.15 (0.06)	1.10 (0.04)	1.07 (0.04)
Fukue	Outflow	87	>3	1.2	0.195 (0.005)	1.57 (0.05)	1.37 (0.05)	1.32 (0.03)	1.21 (0.03)	1.17 (0.03)
Fukue	Outflow	51	<1	19.9	0.182 (0.011)	1.62 (0.09)	1.25 (0.05)	1.24 (0.04)	1.16 (0.02)	1.12 (0.03)
Site	Air mass type	Averaging time* (h)	$\Delta BC/\Delta CO$ ($\text{ng m}^{-3} \text{ppb}^{-1}$)	APT (mm)	Lognormal fit parameters Avg. (1σ)		1-hr median D_s/D_{core} for selected D_{core} Avg. (1σ)			
					MMD (μm)	σ_g	0.15—0.2	0.2—0.25	0.25—0.3	0.3—0.35 (μm)
Yokosuka	Source	184	-	-	0.160 (0.019)	1.84 (0.08)	1.18 (0.07)	1.15 (0.06)	1.10 (0.04)	1.07 (0.04)
Fukue	Outflow	87	>3	1.2	0.195 (0.005)	1.57 (0.05)	1.37 (0.05)	1.32 (0.03)	1.21 (0.03)	1.17 (0.03)
Fukue	Outflow	51	<1	19.9	0.182 (0.011)	1.62 (0.09)	1.25 (0.05)	1.24 (0.04)	1.16 (0.02)	1.12 (0.03)

*Time used for calculating the averaged statistics of the microphysical properties of BC-containing particles.

書式変更: 左 : 35 mm, 右 : 30 mm, 標準の文字数